

SYNTHESIS OF MAPbI_3
SINGLE CRYSTAL BY INVERSE
TEMPERATURE CRYSTALLIZATION AND
CHARGE TRANSPORT STUDIES
BY SCLC METHOD

MASTER OF SCIENCE IN PHYSICS
2020 - 2022

ABSTRACT

Perovskite crystals have received extensive interest in current years because of their facile synthesis and wonderful optoelectronic properties which includes the long carrier diffusion length, high carrier mobility, low trap density, and tunable absorption edge ranging from ultra-violet (UV) to near-infrared (NIR), which give the ability for applications in solar cells, photodetectors (PDs), lasers, etc. Here we are going to discuss the synthesis, properties, and applications of Methylammonium lead iodide perovskite single crystals, particularly through the Inverse Temperature Crystallization method. Methylammonium lead iodide perovskite has been of great concern in recent fields of study. They have a direct band gap of 1.6 eV which suits it as a better option for optoelectronic applications. The absorption range of the MAPbI_3 is very broad. The typical range is from 300 to 800 nm. The longer carrier lifetime and diffusion length of MAPbI_3 perovskite make it an essential one in modern technologies.

The history of the utilization of perovskite structured phases is an object lesson in the value of crystal chemistry. It provides an essential family of materials for a wide variety of present-day technologies and is likely to be an integral part of future developments needed in frequency communication and several other integrated technologies. The diversity of perovskite structure compounds that can be synthesized provides an extreme range of electrical, magnetic, optical, and mechanical properties over a wide temperature range. This could be a special boon to the integrated technologies where the compatibility of the structure of various materials, with different functional properties, is a major concern since the structural mismatch often leads to various aging, failure, and impractical operating limitations for devices. Challenges towards the crystal growth and stability with future scope for the study were also briefly described in the following chapter.

LIST OF FIGURES

| FIG NO | NAME OF FIGURES | PAGE NO |
|-------------|---|---------|
| Figure 1.1 | Ideal cubic perovskite structure | 1 |
| Figure 1.2 | Perovskite crystal | 2 |
| Figure 1.3 | Lev Perovski | 4 |
| Figure 1.4 | Classification of perovskite | 6 |
| Figure 1.5 | Single perovskite | 7 |
| Figure 1.6 | Double perovskite | 8 |
| Figure 1.7 | Layered perovskite | 8 |
| Figure 1.8 | The top-seeded solution growth method | 11 |
| Figure 1.9 | Inverse temperature crystallization | 12 |
| Figure 1.10 | Anti-solvent vapor-assisted crystallization | 13 |
| Figure 1.11 | Cavitation triggered asymmetrical crystallization | 13 |
| Figure 1.12 | Photodetector based on single crystal perovskite | 14 |
| Figure 1.13 | Perovskite solar cell | 15 |
| Figure 1.14 | LED based on perovskite single crystal | 16 |
| Figure 2.1 | Methylammonium lead iodide perovskite | 18 |
| Figure 2.2 | Structure of Methylamine iodide | 19 |
| Figure 2.3 | Methylamine iodide (MAI) precursor salt | 20 |
| Figure 2.4 | Lead (II) iodide precursor salt | 21 |
| Figure 2.5 | Growth of single crystal in oil bath | 22 |
| Figure 2.6 | MAPbI ₃ single crystal | 22 |
| Figure 2.7 | Bragg diffraction in a crystal | 25 |

| | | |
|-------------|--|----|
| Figure 2.8 | Powder XRD | 27 |
| Figure 2.9 | Powder XRD instrumentation set up | 28 |
| Figure 2.10 | UV visible Spectroscopy principle | 30 |
| Figure 2.11 | Dual-beam UV Visible Spectrometer | 31 |
| Figure 2.12 | UV visible Spectrometer | 32 |
| Figure 2.13 | Rayleigh and Raman scattering in molecules | 33 |
| Figure 2.14 | Energy level diagram showing Rayleigh and Raman | 35 |
| Figure 2.15 | Block diagram of Raman Spectrometer | 36 |
| Figure 2.16 | Dispersive Raman spectrometer | 37 |
| Figure 2.17 | FT Raman Spectrometer | 37 |
| Figure 2.18 | Laboratory Raman Spectrometer | 38 |
| Figure 3.1 | Powder XRD of MAPbI ₃ | 44 |
| Figure 3.2 | UV Visible absorption spectrum of MAPbI ₃ | 45 |
| Figure 3.3 | Band gap of MAPbI ₃ | 46 |
| Figure 3.4 | Raman spectrum of MAPbI ₃ | 47 |
| Figure 3.5 | Device structure for iv measurement | 48 |
| Figure 3.6 | SCLC measurement | 48 |

CONTENTS

ABSTRACT

List of figures

CHAPTER 1 - PEROVSKITES

| | | |
|-------|--|----|
| 1.1 | Introduction | 1 |
| 1.2 | Historical aspects of perovskites | 4 |
| 1.3 | Classification of perovskites | 6 |
| 1.4 | Properties of perovskites | 9 |
| 1.4.1 | Dielectric Properties | 9 |
| 1.4.2 | Optical Properties | 9 |
| 1.4.3 | Ferroelectricity | 10 |
| 1.4.4 | Superconductivity | 10 |
| 1.4.5 | Piezoelectricity | 10 |
| 1.4.6 | Catalytic Activity | 10 |
| 1.5 | Synthesis of perovskite single crystal | 11 |
| 1.5.1 | Solution temperature lowering (STL) method | 11 |
| 1.5.2 | Inverse temperature crystallization (ITC) method | 12 |
| 1.5.3 | Anti-solvent vapor-assisted crystallization (AVC) method | 12 |
| 1.5.4 | Thickness controllable methods | 13 |
| 1.6 | Applications of perovskites | 14 |
| 1.7 | Review of literature | 17 |

CHAPTER 2 – MATERIALS AND METHODS

| | | |
|-----------|---|----|
| 2.1 | Methylammonium lead iodide perovskite (MAPbI ₃) | 18 |
| 2.2 | Synthesis technique | 19 |
| 2.2.1 | Precursor salt | 19 |
| 2.2.1.1 | Methylamine iodide (MAI) | 19 |
| 2.2.1.1.1 | Synthesis of Methylamine iodide | 20 |
| 2.2.1.2 | Lead (II) iodide (PbI ₂) | 20 |
| 2.2.1.2.1 | Synthesis of Lead iodide | 21 |
| 2.2.2 | Preparation of precursor solution | 21 |
| 2.2.3 | Growth of single crystal | 22 |

| | | |
|---|--|-----------|
| 2.2.4 | Properties of MAPbI ₃ single crystal perovskite | 23 |
| 2.2.5 | Applications of MAPbI ₃ single crystal perovskite | 23 |
| 2.2.6 | Limitations of MAPbI ₃ single crystal perovskite | 23 |
| 2.3 | Characterisation techniques | 23 |
| 2.3.1 | X- Ray Diffraction | 24 |
| 2.3.1.1 | Fundamental principle of XRD | 25 |
| 2.3.1.2 | Powder X-Ray diffraction | 26 |
| 2.3.1.3 | Instrumentation | 28 |
| 2.3.1.4 | Applications of powder XRD | 29 |
| 2.3.2 | UV Visible Spectroscopy | 29 |
| 2.3.2.1 | Basic ideas of UV Visible spectroscopy | 29 |
| 2.3.2.2 | Instrumentation | 31 |
| 2.3.2.3 | Applications of UV Visible spectroscopy | 33 |
| 2.3.3 | Raman Spectroscopy | 33 |
| 2.3.3.1 | Principles of Raman Spectroscopy | 34 |
| 2.3.3.2 | Instrumentation | 36 |
| 2.3.3.2.1 | Raman Dispersive Spectrometers | 37 |
| 2.3.3.2.2 | FT Raman Spectrometers | 37 |
| 2.3.3.3 | Applications of Raman Spectroscopy | 39 |
| 2.4 | REFERENCE | 40 |
| CHAPTER 3 – RESULTS AND DISCUSSION | | 43 |
| 3.1 | XRD Analysis | 44 |
| 3.2 | UV Visible Absorption spectrum analysis | 45 |
| 3.3 | Raman spectrum analysis | 47 |
| 3.4 | Charge transport studies | 48 |
| 3.5 | Conclusion | 50 |
| 3.6 | REFERENCE | 51 |
| SUMMARY AND SCOPE FOR FUTURE WORKS | | 52 |

CHAPTER -1

PEROVSKITE

1.1 INTRODUCTION

Perovskite is an organic-inorganic hybrid that has the generic form ABX_3 , they have a common structure termed ABX_3 , where “A” and “B” are cations that have different sizes and “X” is an anion that bonds to both. The ‘A’ atoms are bigger than the ‘B’ atoms. The A and B locations may be replaced by any metal or semimetal from the periodic table.

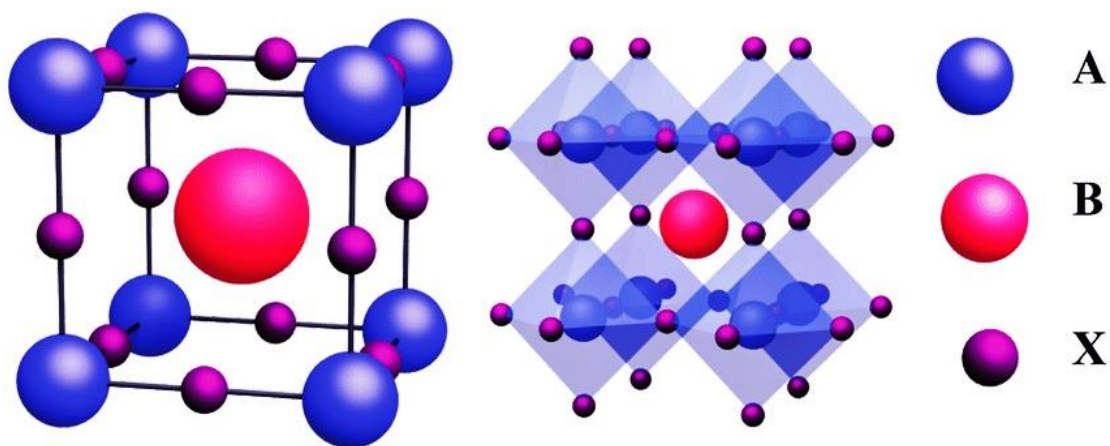


Figure 1.1 - Ideal cubic perovskite structure[1]

The atomic arrangements in perovskite structure were first found for the mineral perovskite calcium titanate, it has a sub-Metallic to metallic luster cube like-structure beside deficient cleavage and hard tenacity, colourless streak or colours include orange, black, brown, yellow, brown, and grey. Ideally, the perovskite structure is described as cubic.

The general formula as ABX_3 , [2] can be explained as; A and B are cations of different sizes and X is the anion. The B atom has 6-fold coordination number and the A atom have 12-fold coordination number. Atom B is found at the corner of the cube and is body-centered, while X atoms are in a face-centered position.

The crystal structure of perovskite can be alternatively viewed as corner-linked BX_6 octahedral with interstitial A cation. The crystallographic stability and apparent structure can be deduced

by considering a Goldschmidt tolerance factor ' t ' and an octahedral factor ' μ '. Here, t is defined as the ratio of the distance A–X to the distance B–X in an idealized solid-sphere model

$$t = \frac{RA+RB}{\sqrt{2} (RB+RX)} \quad [3] \quad (1)$$

where RA , RB , and RX are the ionic radii of the corresponding ions) and ' μ ' is defined as the ratio of the ionic radius of B to the ionic radius of X.

$$\mu = \frac{RB}{RX} \quad (2)$$

The perovskite structure is stable when $0.89 \leq t \leq 1.06$. Ideal cubic structure is only observed at room temperature when t is close to 1. Some changes may exist in perovskite ideal cubic form which leads to the formation of orthorhombic, rhombohedral, hexagonal, and tetragonal forms. For halide perovskites ($X = F, Cl, Br, I$), t and μ have a narrower range, i.e. 0.89–1.0 and 0.4–0.88 respectively.



Figure 1.2 - Perovskite Crystal[3]

Perovskite has a highly stable structure, a large number of compounds with varying properties, and applied applications. The key role includes ferromagnetism and ferroelectricity. The broad formation of solid solutions leads to material optimization by structure control and phase transition engineering.

In the past decade, perovskite materials gained significant development in the photovoltaic and photoelectric fields due to their unique characteristics, such as the tunable bandgap, high absorption coefficient, long charge carrier diffusion length, carrier multiplication, and high carrier mobility making them more advantageous in solar cells. The efficiency of perovskite

solar cells (PSCs) has been enhanced significantly to over 25.2% in the past decade, but the defect dynamics and grain boundaries within the polycrystalline perovskite thin films are major hurdles to further improvement of the efficiency and stability of these devices.

Perovskite single crystals with outstanding photoelectric and optoelectronic properties bring hope due to the low defect density. Studies demonstrate that perovskite single crystals are promising building blocks for photoelectric conversion applications.

The perovskite structure is an extraordinarily versatile one. It provides an essential family of materials for a wide variety of present-day technologies and is likely to be an integral part of the future developments needed in high-frequency communication and several other integrated technologies. The diversity of perovskite structure compounds that can be synthesized, provides the extreme range of electrical, magnetic, optical, and mechanical properties over a wide temperature range. This could be a special boon to the integrated technologies where the compatibility of the structure of various materials, with different functional properties, is a major concern since the structural mismatch often leads to various aging, failure, and impractical operating limitations for devices.

By using the vast crystal chemistry resources and principles (e.g., ionic radii, valence, tolerance factor, etc.) innumerable perovskite compounds with a variety of properties can be designed. Several highly technologically important properties from macro to nanoscale have already been identified in this class of materials. Perovskite structure compounds are and will be an integral part of the important commercial and strategic technologies of the future.

1.2 HISTORICAL ASPECTS OF PEROVSKITES



Figure 1.3 - Lev Perovski [4]

“Perovskite” is the name of a crystal structure, which was found by a Russian scientist, Lev Perovski. The structure was based on a cubic structure and was composed of three elements as ABX_3 . The oxide perovskite, which has been a famous crystal and ceramic for Scientists and is quite stable against circumstance was found by Lev Perovski composing 2+ metal cation in the A site, 4+ metal cation in the B site, and 2- oxygen anion in the O site. The most famous perovskite crystals are $CaTiO_3$ and $BaTiO_3$.

The mineral was discovered in the Ural Mountains of Russia by Gustav Rose in 1839. Afterward, Wells found another style of perovskite crystal, composed of 1+ alkaline cation (Cs^+ and K^+), 2+ lead cation (Pb^{2+}), and 1- halogen anion (I^- , Br^- , and Cl^-) in 1893.

Perovskite’s notable crystal structure was first described by Victor Goldschmidt in 1926 in his work on tolerance factors.[8] The crystal structure was later published in 1945 from X-ray diffraction data on barium titanate by Helen Dick Megaw. In 1978, Weber found the possibility of utilization of methyl ammonium cation ($CH_3NH_3^+$) for the components in lead-halide perovskite crystals. In 1995, Mitzi et al. Reported the 2-dimensional organo-lead-halide perovskite crystal with a special function of semiconducting in science resulting in a big impact on the scientific society and a big Research project in Japan (CREST).

Historically, however, perovskite would have remained a Mineralogical curiosity were it not for V.M. Goldschmidt, the founder of the science of crystal chemistry. and his school of geochemists in Oslo. Goldschmidt made and studied a large number of the first synthetic Verbindung perovskites with different compositions, including $BaTiO$, in 1924-26. This

quotation is taken from Goldschmidt's classic, the single most important reference in the entire history of materials synthesis, entitled "Geochemische Verteilungsgesetze der Elemente":

But not only did Goldschmidt synthesize many such isostructural phases but he started what was to become the world's first school of crystal chemistry by determining the crystal structures of each of the phases of the ABX_3 compositions. This was in an era when powder x-ray diffraction was in its infancy. Goldschmidt then went on to establish what remains after seventy-five years the first (and lasting) principles of materials synthesis. The perovskite structure was central to the birth of these ideas where Goldschmidt introduces the concept of the "tolerance factor" (T.F.)

Perovskites (organic-inorganic) have reached the top position within ~5 years, due to substantial improvement in power conversion efficiency and low processing costs in the modern era.[5] They have a significant impact on photovoltaic devices and the solar-to-Power conversion efficiency is considerably high (~20.1%) compared to the existing organic solar cells and dye-sensitized solar cells. Nevertheless, some issues need to be addressed to commercialize the perovskite Solar cells. Particularly, the stability of these cells is not well documented.

1.3 CLASSIFICATION OF PEROVSKITE

Perovskite or perovskite-structure are used interchangeably. This name is given to anything that has the generic form ABX_3 and the same crystallographic structure.[6]

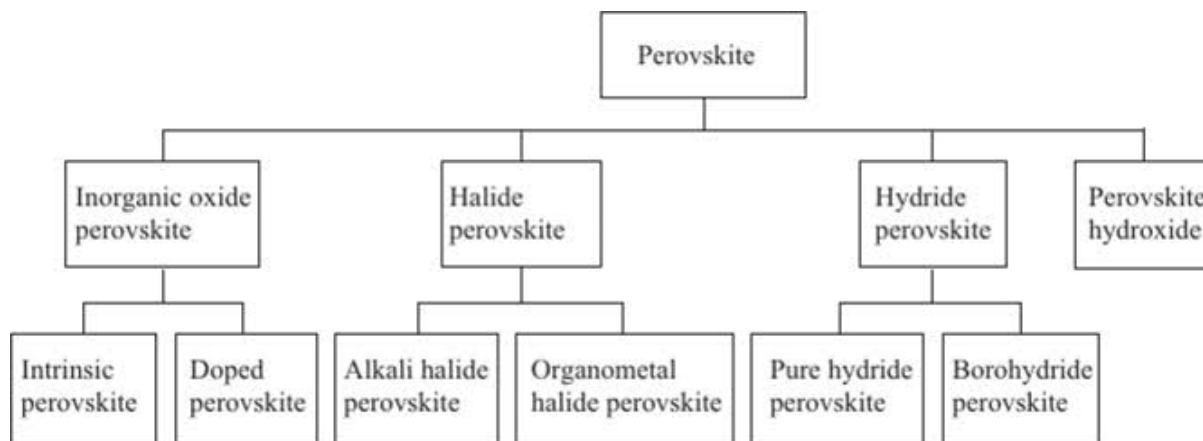


Figure 1.4 Classification of perovskites

- **Inorganic oxide perovskites** - Inorganic oxide perovskites, including intrinsic perovskites and doped perovskites in terms of chemical elements on their specific sites. Often, the inorganic perovskite oxides deviate from the ideal cubic structure depending on the size of A- and B-site cations, additionally such structural changes are sensitive to temperature and sometimes pressure, resulting in a subsequent change in the properties. The oxygen vacancies of oxide perovskites are unique.
- **Halide perovskite** - Halide perovskites, including alkali halide perovskites and organometal halide perovskites. The attempts are also made to synthesize perovskite structured fluorides with the general formula AMF , (where $A = Na, K, Cs, Rb$, etc., $M = Mn, Fe, Co, Ni, Zn, Mg, Cu$, etc.). Generally, these perovskite fluorides exhibit antiferromagnetic properties, and some of them are identified as excellent hosts for luminescent ions. Perovskite structured halides with the general formula ABX , (where $A = Cs, B = Pb, Sn, X = Cl, Br$, and Cl) gained remarkable attention because of their superior optical properties as compared to many organic small molecules.
- **Hydride perovskite** - Hydride perovskites, including $ABXr$ type pure hydride perovskites, such as $MgXH$, ($X = Fe, Co$) and borohydride perovskites $AS(BH_4)_3$.

Hydride perovskites are formed when the stoichiometric ratio of the hydrides of A- and B-site cations are heated (~ 673 K) under a high-pressure atmosphere. This process is reversible. Therefore, these materials are extensively studied as hydrogen storage materials.

- **Perovskite hydroxide** - Perovskite hydroxide adopts the formula $AB(OH)_6$ with a double perovskite structure. These materials exhibit catalytic properties due to their unique optical and electronic properties. Some of the examples are, $ASn(OH)_6$ ($A=Mg, Sr, Ba, Zn, Cu, Co, Fe, Mn, \text{etc.}$)[6]

In terms of perovskite structures, perovskites can be classified as

1. **Single perovskites** - The single perovskites adopt a low symmetrical triclinic to high symmetric cubic phases. They are the most studied perovskites, and their properties can be easily modified by doping.

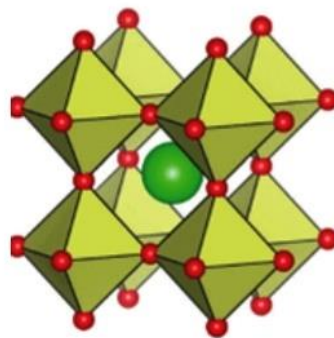


Figure 1.5 – Single perovskite[7]

Single perovskite oxide structures with alkaline earth metal or rare earth metals at the A-site and transition metal at the B-site are the most studied among single perovskites. Unlike complex perovskites, most single perovskites can be synthesized easily at low temperatures using conventional technique

2. **Double perovskites** - Double perovskites with the formula AB_2X_6 are also successfully synthesized following the advantages of ABX_3 perovskite structured materials. The presence of two property determining B-site cations is likely to exhibit superior properties than ABX_3 perovskite materials, especially among the halide perovskites for

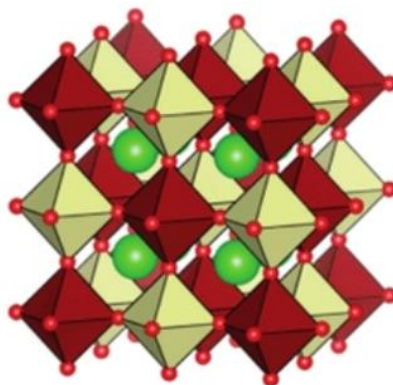


Figure 1.6 – Double Perovskite[7]

optoelectronic applications. Some double perovskite oxides outperform single perovskites in electrocatalysis water splitting and thermoelectric properties to the commercial noble metal and chalcogen-based materials.

3. **Layered perovskites** - The layered perovskites are further classified as the Ruddlesden-Popper phase, the Dion-Jacobson phase, the Aurivillius phase, and $A_nB_{n+2}O_{3n+8}$ layered phase. Layered perovskites are useful materials that contain sheets

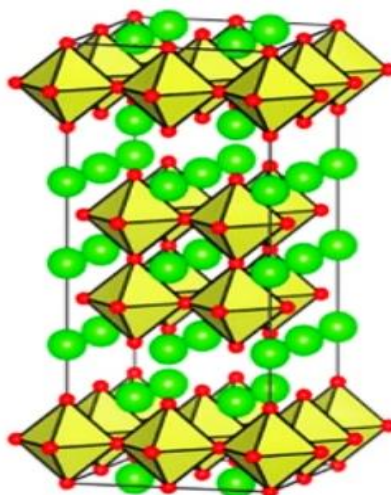


Figure 1.7 – Layered perovskite[7]

of a perovskite semiconductor enclosed by organic molecules. Layered hybrid perovskites (LPKs) have emerged as an answer to battle stability concerns. They exhibit exceptional characteristics, such as superconductivity, that are not observed in single or double perovskite counterparts, due to the oxygen-rich separating layers between the perovskite slabs. Although known for decades, LPKs have only recently been incorporated in photovoltaic (PV) applications, resulting in modest device power conversion efficiencies due to poorer optoelectronic properties

1.4 PROPERTIES OF PEROVSKITES

Perovskite materials exhibit many interesting properties due to its characteristic chemical nature such as their non-stoichiometry of the anions and/or cations, the valence mixture electronic structure, the distortion of the cations etc.[8]

1.4.1 Dielectric Properties - Dielectric materials are the materials in which electro-static fields can persevere for a long time. Layers of these substances are generally inserted into capacitors to improve their performance, and the term dielectric refers to this application. Great dielectric permittivity or ferroelectric materials are of massive importance as electro ceramics for the engineering and electronics industry. Several routes have been pursued to explain the dielectric and mechanical properties starting from the simple structure BaTiO_3 by the solid solution system $\text{Pb}(\text{Zr,Ti})\text{O}_3$ to other distinct families of materials. These routes care about the flexibility of chemical manipulation and submissiveness of the perovskites.

1.4.2 Optical Properties - Perovskites provide a very special class of materials with excellent optical and photoluminescence properties. The optical density of CaTiO_3 showed absorption characteristics quite similar to those of SrTiO_3 crystals with the exception that the absorptions are shifted to short-wavelength. Both of these compounds have been considered for high-temperature infrared windows. SrTiO_3 is considered as an excellent material for use with optically immersed infrared detectors. Some perovskite's electro-optic coefficients of are nearly constant with temperature. Potassium tantalate niobate (KTN) is one of the perovskite oxides which has a large room temperature electro-optic effect and wide-angle fast optical beam scanner,

therefore this type is not only useful to optical communications, but also to various other products that use optical beams, such as laser applications.

1.4.3 Ferroelectricity - Ferroelectricity is the phenomenon that occurs when an external electric field is applied to some materials leading to a spontaneous electric polarization. The discovery of ferroelectricity in perovskite-based materials and another barium titanate (BaTiO_3) opened up new different application for ferroelectric materials, leading to significant interest in other types of materials. Ferroelectric property is used to several purposes such as; in ultrasound imaging devices, fire sensors, infrared cameras, vibration sensors, tunable capacitors, memory devices, RAM and RFID cards, input devices in ultrasound imaging, and a. make sensors, capacitors, memory devices, etc.

1.4.4 Superconductivity - Certain materials once cooled under a specific serious temperature exhibited zero electrical resistance and expulsion of magnetic flux fields this phenomenon is called Superconductivity. The oxide perovskite's structure type provides an excellent structural framework due to the existence of superconductivity. Perovskites that have Cu act as high-temperature superconductors. The first reported example of superconducting perovskites is La-Ba-Cu-O perovskite and there are many more. Perovskite oxides now eclipsed the use of Intermetallic compounds as a source of many superconducting materials such as; cesium tungsten bronzes and Sodium, potassium, rubidium, etc.[9]

1.4.5 Piezoelectricity - Some materials have the capacity to produce an electric charge in reaction to applied mechanical stress is known as Piezoelectricity. Therefore, if definite crystals were subjected to mechanical strain, they became polarized at a degree which is proportional to the applied strain. On the other hand, they have some changes when they are exposed to an electric field which is known as the inverse piezoelectric effect. Piezoelectricity properties have many valuable scientific applications such as; Cigarette lighters, Sensors, Microphones, High voltage, and power sources, Pick-ups, Pressure sensors, Force sensors, Strain gauges, Actuators, Piezoelectric, etc.[9]

1.4.6 Catalytic Activity - Perovskites displayed exceptional catalytic action and great chemical stability therefore it includes in the catalysis of changed reactions. The

perovskite structure showed high catalytic activity in addition their stability allowed the preparation of several compounds from elements with uncommon valence statuses or a great extent of oxygen lack.

1.5 SYNTHESIS OF PEROVSKITE SINGLE CRYSTAL

The controllable synthesis of high-quality perovskite single crystals is of fundamental importance for their applications while the methods used at earlier stages for the synthesis of perovskite single crystals were time-consuming and challenging. To obtain desired dimensions and properties, the effects have been devoted to developing more efficient synthesis methods for improving crystal quality. Whereas high-quality and large-size crystals are still difficult to obtain.[10]

1.5.1. Solution temperature lowering (STL) method - The solution temperature lowering (STL) method stems from Weber's method, which utilizes the difference in solubility of the perovskite precursors in solvents under different temperatures. The perovskite precursors are dissolved into the solvents at higher temperatures, then the temperature of the solution is gradually reduced to reach a supersaturated state which results in the growth of single crystals. Besides the examples of the bottom-seeded STL method as described above perovskite single crystals can also be grown by the top-Seeded solution-growth (TSSG) .[11]

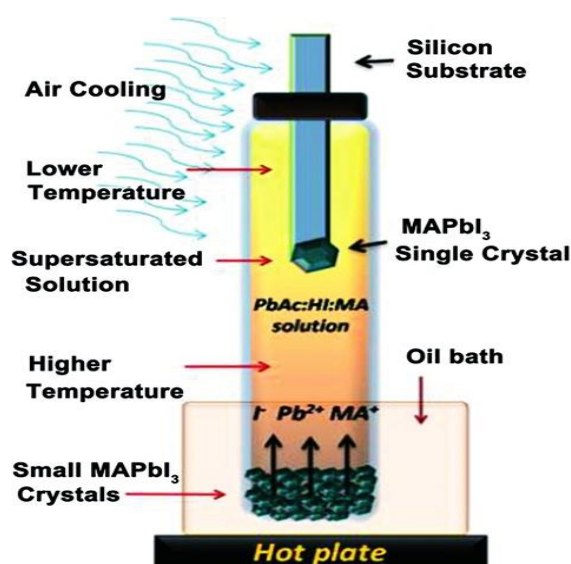


Figure 1.8 – Top-Seeded Solution Growth Method (TSSG)[12]

1.5.2 Inverse temperature crystallization - In the process of the inverse temperature crystallization (ITC) method, the precursor solution was put in a bottle and heated at a fixed temperature to grow single crystals. During the growth process, in the beginning, the surface of the solution is in a saturated state because of the volatilization of the solvent, while the bottom of the solution is

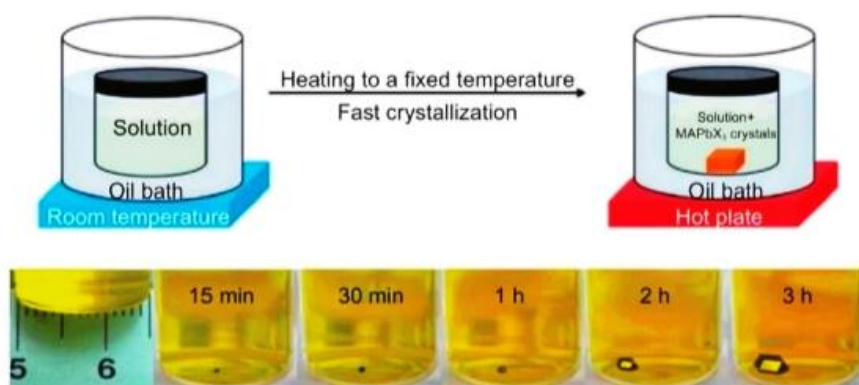


Figure 1.9 – Inverse Temperature Crystallization method

unsaturated. As the solvent decreases, the concentration will exceed the solubility of precursors because of the convection inside the bottle, which leads to the growth of single crystals. The pre-synthesized seed is used as a nucleation site for the growth of large single crystals. If the temperature is higher, but the crystal will be malformed or small crystals will be formed when the temperature is too high. It should be noted That the crystal will be re-dissolved if the temperature decreases to room temperature. Therefore, the single crystals should be harvested before cooling the solution. This method is suitable for the preparation of multi-component single crystals.

1.5.3 Anti-solvent vapour-assisted crystallization (AVC) method - The anti-solvent vapor-assisted crystallization (AVC) is a reproducible and temperature-independent method to grow high-quality single crystals by utilizing the solubility of the precursor solution in different solvents. It was developed by Bakrs group to grow crack-free MAPbBr₃ single crystals with a volume exceeding 100 mm³. The precursor is put into a sealed bottle containing antisolvent,

and the solubility of the mixed solvent decreases when the antisolvent is diffused into the precursor solution, resulting in the growth of crystals.

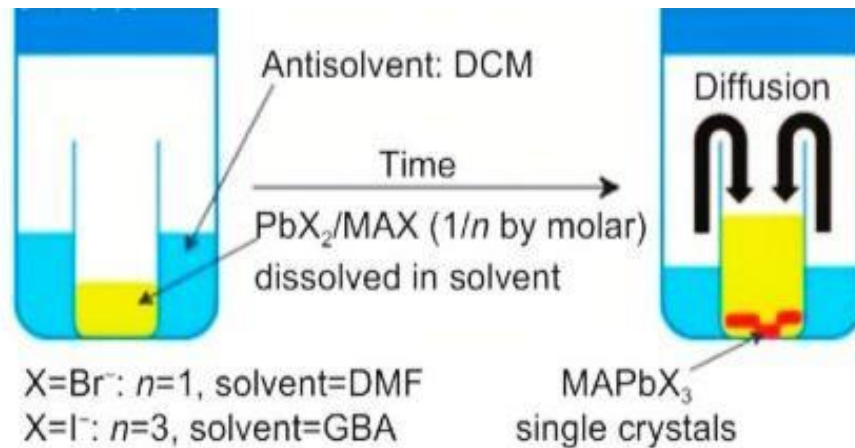


Figure 1.10 Anti – solvent vapour assisted crystallisation[12], [13]

1.5.4 Thickness controllable methods - With the development of preparation methods for perovskite single crystals, controlling the thickness has become a challenge, because the thickness of single crystals influences the device application significantly. The thickness controllable methods of single crystals mainly include the cavitation-triggered asymmetrical crystallization (CTAC) strategy, facile solution-processes method, vertical Bridgman technique, space-limited inverse temperature crystallization (SLITC) etc.

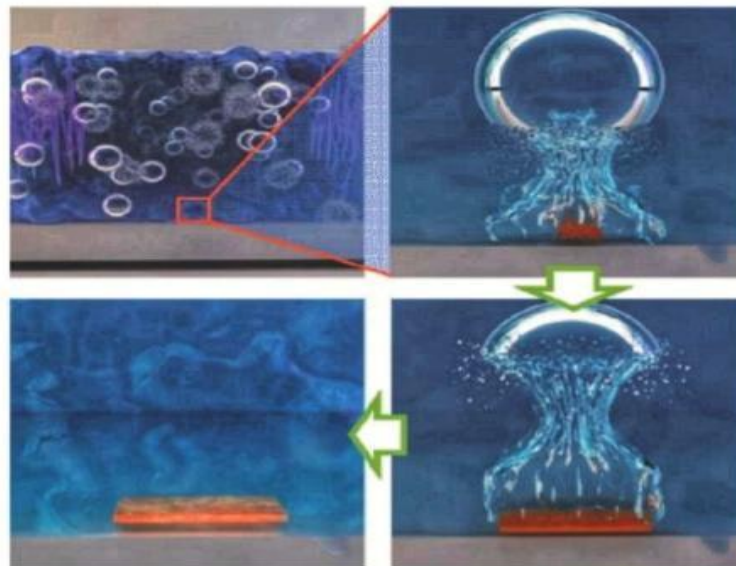


Figure 1.11- Cavitation-triggered asymmetrical crystallization (CTAC) strategy

The large bulk and uneven distribution on the surface of single crystals hinder the further research, which is due to the higher nucleation energy barrier. Through ultrasonic pulses, the nucleation on the surface was promoted on the low super saturation level, increasing the pressure and energy accumulation, which is attributed to the cavitation process. The strong shearing force will control the thickness within a certain range.[9]

1.6 APPLICATIONS OF PEROVSKITES

Perovskite thin films with outstanding photovoltaic properties show advantages in applications, such as PDs , solar cells, Lasers , and LEDs. In contrast, single crystals have great potential due to the superior features. The architecture of single-crystal devices includes vertical and lateral structures. Among them, the latter overcomes the obstacles that the thickness of single crystals brings and shows diverse applications.[8]

- **Photodetectors (PDs)** - Perovskite PDs can be implemented in camera imaging, communications, medical equipment, etc, which can convert light signals to electronic signals. The responsivity (R) and EQE are basic parameters to evaluate PDs. R is a critical parameter that describes the response efficiency of optical to electronic signals, reflecting the efficiency of response to the optical signal. R is defined as the proportion of the photocurrent to incident light intensity, EQE is the value that transforms the photons to charge carriers (electrons and holes).MAPbBr₃ single-crystal PDs not only can detect visible light but also are sensitive to X-rays .It is demonstrated that the MAPbBr₃ single crystals show a high $\mu\tau$ product and low surface recombination velocity, which contribute to the sensitive X-ray detectors.[14]

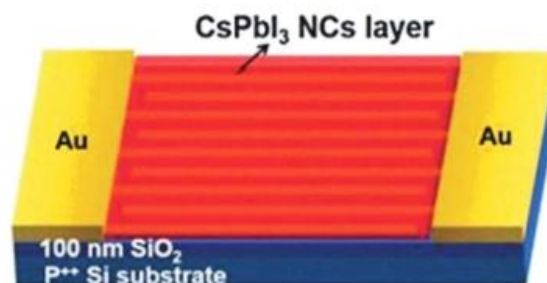


Figure 1.12 – Photodetector based on single crystal perovskite

- **LASER** -The lasers based on perovskite semiconductors show low amplified spontaneous emission (ASE) due to the outstanding characteristics including large absorption coefficients, tunable emission wavelength peaks, low trap density, and low Auger recombination. In contrast to 3D Perovskite thin films, nanoparticles, nanoplates, and nanocrystals form a natural resonant cavity to achieve population inversion required for ASE and lasing. Lasers fabricated by perovskite single crystals have garnered huge attention of researchers as it showed outstanding performance, including optical-gain media, spectrally narrow gain profiles, high quality factors, and low lasing thresholds.
- **Solar cells** - One of the green sources of energy is solar energy because it can be used to replace the fossil fuels. Solar radiation can be transformed to electrical energy in a suitable way. It can be perfectly changed into electricity using photovoltaic solar cells which can be built on silicon. The disadvantage of silicon built solar cell is high price of electricity

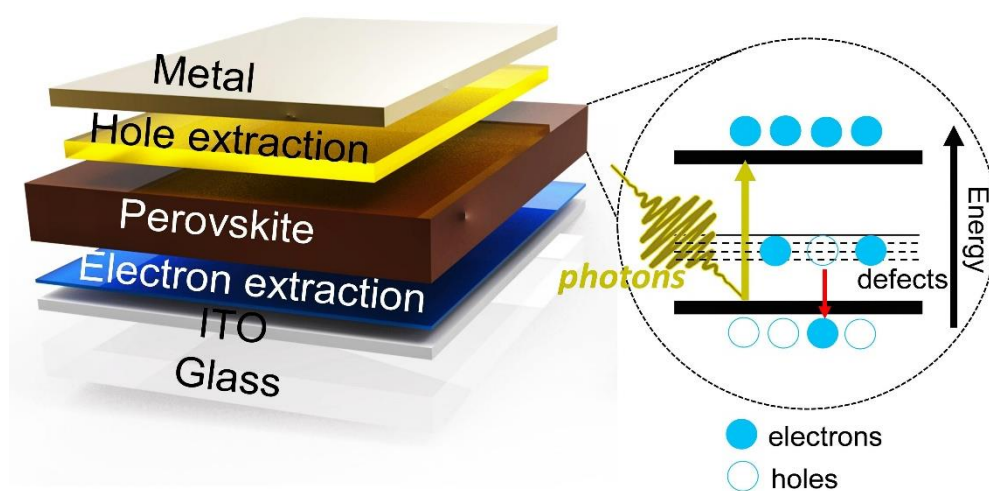


Figure 1.13 – Perovskite Solar cell

produced from it, so develop solar cell with low cost is needed. Solar cells created on organic/ inorganic solid-state methylammonium lead halide hybrid perovskite are in used because it presented better points such 20% lower cost than that of traditional silicon solar cells in addition to the availability of the raw materials. Perovskite showed outstanding essential properties for photovoltaic applications like suitable band gap excellent stability, long hole-electron diffusion length, high absorption coefficient, high carrier mobility & transport, low temperature of processing, charge carriers with small effective mass and easy processing steps.

- **Light emitting diodes (LEDs)** - The electroluminescence (EL) property of perovskite semiconductors was first demonstrated in 1994 by Era et al., but the process can only be operated in liquid-nitrogen temperature [85]. Therefore, a high-quality perovskite layer is essential for fabricating efficient LEDs. Until 2014, Tan et al. prepared perovskite LEDs based on MAPbBr₃ thin films found at the green range, as well as MAPbI_xCl_{1-x} found at the infrared range which are operational at room temperature instead of air. Whereas, this still creates stumbling blocks for applications. Perovskite single crystalline MAPbBr₃ nanoplates produced by the modified ligand-assisted precipitation method showed enhanced moisture resistance caused by hydrophobicity at the end of the long chains, bringing promise for LED devices.[15]

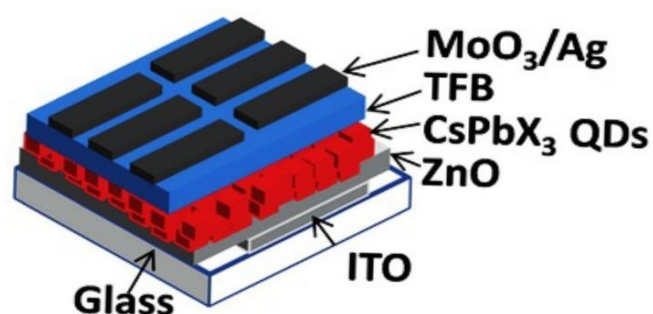


Figure 1.14 – LED based on Perovskite single crystal

- **Sensors and biosensors** - Perovskites materials which contain cobaltite's, titanates, and ferrites were applied as gas sensors for spotting CO, NO₂, methanol, ethanol, and hydrocarbons. Glucose is the basic metabolite in many of the living organisms and in clinical check of diabetes mellitus, and universal Healthiness problem Although there are different types of enzymatic work as glucose sensors but these enzyme lack the stability due to its basic nature in addition its action was greatly affected by poisonous chemicals, temperature, humidity, etc. consequence, there must be searching for stable, sensitive, simple, and selective non-enzymatic glucose sensor such as inorganic perovskite oxides. This sensor have perfect electrocatalytic activity toward glucose in alkaline medium due to the occurrence of huge amount of active sites in the modifier.

1.7 REVIEW OF LITERATURE

- **1..Eman Abdul Rahman Assirey** – This paper analyses perovskite organometallic halide that showed efficient essential properties for photovoltaic solar cells. The review presents a full coverage of the structure, progress of perovskites and their related applications. The unique perovskite structure has the potential to provide a wealth of novel compounds based on A and B site occupancy, which gives rise to a wide range of materials systems with unique properties and wide applications. Several methods were used as synthesizing methods of perovskites compounds are mentioned. The variety of perovskite compounds synthesizing methods provided materials for many commercial and special technologies in addition to great range of electrical, magnetic, optical and mechanical properties over a wide-ranging temperature.
- **2.Shan-Shan Rong ,M. Bilal Faheem, Yan-Bo Li** – This paper presents the properties of perovskite crystals that have gained enormous attention in recent years due to their facile synthesis and excellent optoelectronic properties including the long carrier diffusion length, high carrier mobility, low trap density, and tunable absorption edge ranging from ultra-violet (UV) to near-infrared (NIR), which offer potential for applications in solar cells, photodetectors (PDs), lasers, etc. Along with the properties applications of organic inorganic mixed and all-inorganic perovskite single crystals, particularly through the solution synthesis approach. Challenges towards the crystal growth and stability with future perspectives were also briefly described at the end of this manuscript.
- **3.A.S. Bhalla, Ruyan Guo , Rustum Roy** - The perovskite structure is shown to be the single most versatile ceramic host. By appropriate changes in composition one can modify the most significant electro- ceramic dielectric (BaTiO), and its relatives) phase in industry, into metallic conductors, superconductors or the highest-pressure phases in the earth. After an historical introduction of the science, detailed treatment of the applications is confined to the most recent research on novel uses in piezoelectric, ferroelectric and related applications. In this article, several highly technologically important properties from macro to nanoscale have already been identified in this class of materials. The paper presents perovskite structure compounds as an integral part of the important commercial and strategic/special technologies of the future.

CHAPTER - 2

MATERIALS AND METHODS

This chapter deals with the synthesis methods, materials used and characterization techniques for analysing the single crystals grown. Detailed Information about the crystals is provided along with structural properties and applications of each material used in the synthesis.[11]

2.1 METHYLAMMONIUM LEAD IODIDE PEROVSKITE (MAPbI₃)

Methylammonium lead iodide (MAPbI₃) are solid compounds with perovskite structure and a chemical formula of CH₃NH₃PbI₃ . The material is composed of three ion types: positively charged methylammonium (MA, a polyatomic organic ion), lead and negatively charged iodide.

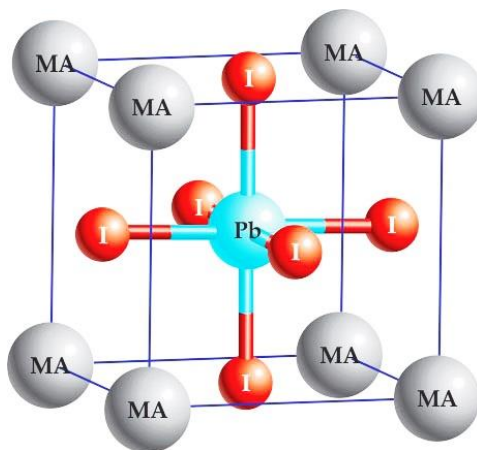
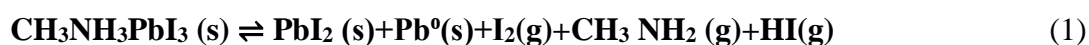


Figure 2.1 - Methylammonium lead iodide perovskite

They belong to the group of organic - inorganic halide perovskites (OIHPs) that exhibit exceptional electrical and optical behaviour suitable for photovoltaic applications. However chemical stability of perovskite crystal has to be improved for efficient optoelectronic communications. In perovskite solar cell researchers proposed the decomposition of MAPbI₃ in the presence of water releasing CH₃NH₂ and HI gases. Furthermore, at low temperature conditions (< 100 °C) compatible with photovoltaic operation found that CH₃NH₃PbI₃ undergoes reversible chemical decomposition.



I₂ gas is released from MAPbI₃ even in dark conditions during mild heating which correspond to solar cell working temperatures.

2.2 SYNTHESIS TECHNIQUE

MAPbI₃ single crystal perovskite was synthesized using Inverse Temperature Crystallization (ITC) method at open room conditions.

Inverse Temperature Crystallization (ITC) method is one of the faster methods to grow single crystals of perovskites like MAPbI₃, comparing with other methods. Techniques like Solution Temperature Lowering method (STL) or Anti-solvent Vapour Assisted Crystallization (AVAC) is time consuming and require more amount of time to grow a single crystal of desired volume. ITC method utilises the retrograde solubility of perovskite in specific solvents. Normally the solubility of a given solute in a given solvent increases with temperature but some solutes become less soluble as temperature increases this inverse temperature dependence referred to as retrograde or inverse solubility. Thus the dissolution of a salt showing retrograde solubility in a given salt is exothermic in nature.

2.2.1 PRECURSOR SALT

Synthesis of MAPbI₃ contains two precursor salts -

- Methylamine iodide (MAI)
- Lead(II) iodide (PbI₂)

2.2.1.1 METHYLAMINE IODIDE (MAI)

Methylammonium iodide is an organic halide with a formula of CH₆IN. It is an ammonium salt composed of methylamine and hydrogen iodide with IUPAC name Methylazanium iodide. It is one of the most common precursors used in the preparation of perovskite. MAI has a molar

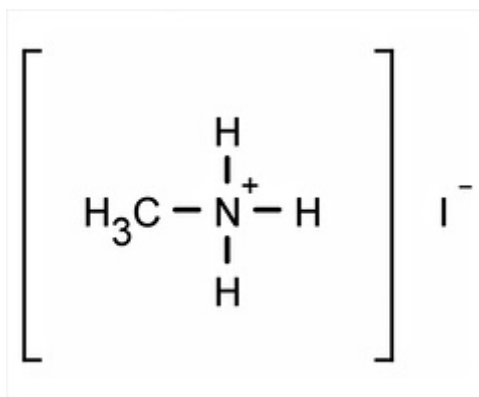


Figure 2.2 Structure of Methylamine iodide

mass of 158.970 g/mol with topological polar surface area of 27.6 Å². Physical Appearance of MAI is white crystalline form with a purity of 99.9 % as per elemental analysis.

The hydrogen bonds are found to be the major factor that stabilizes the methylammonium iodide monomers and dimers, while the dimeric structure exhibits geometry with each iodine atom shared by two neighbouring hydrogen atoms in the methylammonium cation molecules.

2.2.1.1.1 SYNTHESIS OF METHYLAMINE IODIDE (MAI)

Methylamine iodide (MAI) was synthesized by reacting 35 ml of methylamine and 37 ml of Hydroiodic Acid (HI) in a beaker at 0° Celsius for 2 h with constant magnetic stirring. An orange-yellow coloured powder is obtained when the above-mentioned solution is evaporated using a rotavapor at 75°C for 3 h. The synthesized powder is dissolved in Ethanol and recrystallized using diethyl ether and washed three times with diethyl ether. Thus produced MAI was dried at 60°C in vacuum overnight, and the final product in the form of white methylamine iodide powder was saved at 25°C in a desiccator.[6]



Figure 2.3 Methylamine iodide (MAI) precursor salt

2.2.1.2 LEAD(II) IODIDE (PbI₂)

Lead(II) iodide formerly called plumbous iodide with chemical formula PbI₂ with a molar mass of 461.01 g/mol. It is a precursor material in the fabrication of highly efficient solar cells. Hexagonally shaped crystal structure PbI₂ is a bright yellow odourless crystalline solid at room temperature and becomes orange and red when heated with a density of 6.16 g/cm³.

2.2.1.2.1 SYNTHESIS OF LEAD IODIDE

PbI₂ is commonly synthesized via a precipitation reaction between potassium iodide KI and lead(II) nitrate Pb(NO₃)₂ in water solution.

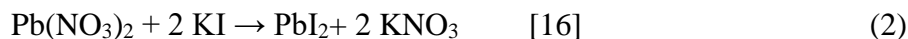


Figure 2.4 Lead (II) iodide precursor salt

2.2.2 PREPERATION OF PRECURSOR SOLUTION

Precursor solutions of different concentrations were prepared by mixing fixed amounts of synthesized MAI and PbI₂ in gamma- Butyrolactone (GBL). Synthesised MAI with molar mass of 158.9695 g/mol and molarity 1.23 M is made up to 5 ml in a beaker. The total mass of methylamine iodide used for the preparation of precursor solution was 2.8352 g. PbI₂ with a molar mass of 461.01g/ mol is made up to desired of 5ml having molarity 1.23 M. The total mass of Lead iodide used for the preparation is 0.9776g.

- Molecular weight of MAI = 158.9695 g/mol
Desired final volume of MAI solution = 5 ml
Molarity = 1.23 M
Mass of Methylamine iodide = 2.8352 g
- Molecular weight of PbI₂ = 461.01 g/mol
Desired final volume of PbI₂ = 5 ml
Molarity = 1.23 M
Mass of Lead iodide = 0.9776 g

2.2.3 GROWTH OF SINGLE CRYSTAL

The mixture of a stoichiometric amount of MAI and PbI_3 in GBL solvent was placed at 60°C for 10 h with constant magnetic stirring in a magnetic stirrer. Then 5 ml of the solution was maintained at different temperatures from 90°C to 110°C on a hot plate for 48 h for the single crystals to grow in the solution.



Figure 2.5 - Growth of Single Crystal in oil bath

To ensure uniform temperature during the course of crystal growth, silicon oil bath is used to maintain the growth solution at desired temperatures. Crystal taken from oil bath. After washing with isopropanol and diethyl ether MAPbI_3 single crystal perovskite is obtained and used for further analysis.

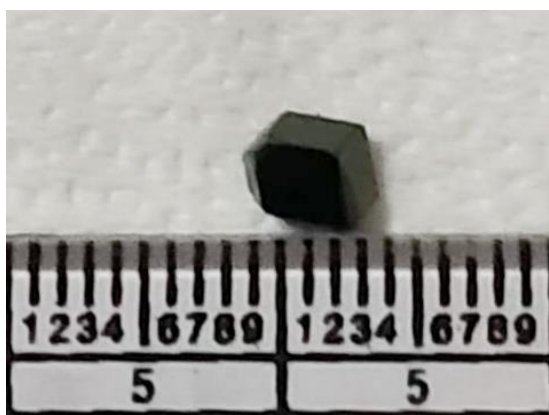


Figure 2.6 MAPbI_3 single Crystal

2.2.4 PROPERTIES OF MAPbI₃ SINGLE CRYSTAL PEROVSKITE

Methylammonium lead iodide perovskite has attracted its importance in many emerging field of interests. Certain properties of MAPbI₃ has got greater importance in future technologies. They have a direct band gap of 1.6 eV making it a better option for optoelectronic applications. The absorption range of the MAPbI₃ is very broad the typical range is from 300 to 800 nm. Longer carrier lifetime and diffusion length of MAPbI₃ perovskite marks its importance in modern technologies.

2.2.5.APPLICATIONS OF MAPbI₃ SINGLE CRYSTAL PEROVSKITE

The solar-to-power conversion efficiency of MAPbI₃ is considerably high about (~20.1%) making it a better option for all electronic instruments. MAPbI₃ is an alternative to silicon solar cells which have been developed based on various dye sensitizers, organic and hybrid (organic–inorganic) materials. Another important aspect is high charge-carrier mobility, which is more useful for developing high-performance solar cell devices.

2.2.6 LIMITATIONS OF MAPbI₃ SINGLE CRYSTAL PEROVSKITE

MAPbI₃ are significant for research and commercialization of solar cells in the next few years due to high efficiency and durability. However, toxicity of lead is a major concern which easily degrades on exposure to humidity and ultraviolet (UV) irradiation. Utilization of Pb-based materials in solar cells is restricted due to their toxicity. For commercialization of a Perovskite Solar Cell (PSC) solar device, stability is a major issue. Although few reports highlight controlling the device stabilities other concerns like intrinsic stabilities at the interface and device architecture remain major obstructions to practical applications.\

2.3 CHARACTERISATION TECHNIQUES

Characterization techniques essentially involves the evaluation of the chemical composition, structure, optical, mechanical, electrical and thermal properties of the grown crystals. Different types of characterization techniques are available to study the physical and chemical properties of the crystal. There are number of experimental techniques used in the present investigation to characterize the properties of the grown single crystals such structural (XRD), thermal (TGA/DSC), optical (UV-Visible), vibrational (Raman), hardness and dielectric measurements.

The selectivity of method depends upon the type of the sample, information required, time constraints and the cost of analysis. For studying single crystals parameters are identified and database are collected and tabulated for further studies.

In this section we shall discuss in detail about structural, optical & thermal analysis techniques used to analyse MAPbI₃ single crystal perovskite.

| Analysis Parameter | Technique used |
|------------------------|--------------------------|
| Structure | Powder X-Ray Diffraction |
| Optical Properties | U.V Visible Spectroscopy |
| Vibrational properties | Raman Spectroscopy |
| Mobility | Charge transport studies |

Table -1

2.3.1 X RAY DIFFRACTION

X-ray diffraction (XRD) is a famous structural analysis technique used for the primary characterization of material properties like crystal structure, crystallite size, and strain. This test method is performed by directing an x-ray beam at a sample and measuring the scattered intensity as a function of the outgoing direction. Once the beam is separated, the scatter, also called a diffraction pattern, indicates the sample's crystalline structure.

X-rays are a form of electromagnetic radiation, similar to visible light. Unlike light, however, x-rays have higher energy and can pass through most objects, including the body with

wavelength range of 1 \AA . X-rays can be generated by an X-ray tube, a vacuum tube that uses a high voltage to accelerate the electrons released by a hot cathode to a high velocity. Accelerating electrons with high voltages are allowed to collide with a metal target. If the bombarding electrons have sufficient energy, they can knock an electron out of an inner shell of the target metal atoms then the electrons from the higher states drop down to fill the vacancy, emitting x-ray photons with precise energies determined by the electron energy levels. These rays are called characteristic x-rays.[17]

XRD pattern is very useful in several ways -

- Identifying compounds under investigation.
- Evaluation of the lattice strain in case material is deformed.
- Measurement of lattice parameter from the peaks.
- Identify crystal structure and density of compounds after mapping with JCPDS (Joint Committee on Powder Diffraction Standards) data bank.

2.3.1.1 FUNDAMENTAL PRINCIPLE OF XRD

Crystals are regular arrays of atoms, whilst X-rays can be considered as waves of electromagnetic radiation. Crystal atoms scatter incident X-rays, primarily through interaction with the atoms' electrons. This phenomenon is known as elastic scattering; the electron is known as the scatterer. A regular array of scatterers produces a regular array of spherical waves. In the majority of directions, these waves cancel each other out through destructive interference, however, they add constructively in a few specific directions.

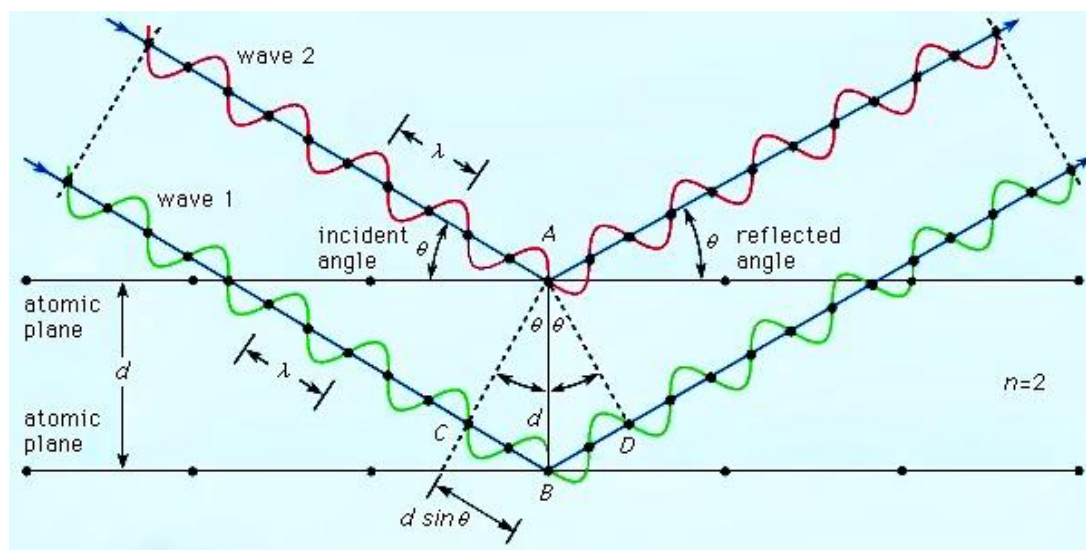


Figure 2.7 – Bragg Diffraction in a crystal

In figure 2.6 , waves 1 and 2, in phase with each other, glance off atoms A and B of a crystal that has a separation distance d between its atomic, or lattice, planes. The reflected (glancing) angle θ , as shown by the experiment, is equal to the incident angle θ . The condition for the two waves to stay in phase after both are reflected is that the path length CBD be a whole number (n) of wavelengths (λ), or $n\lambda$. But, from geometry, CB and BD are equal to each other and to the distance d times the sine of the reflected angle θ , or $d \sin \theta$. Thus,

$$n\lambda = 2d \sin \theta \quad (3)$$

where d – spacing between atomic planes. The above equation is known as Braggs law of Diffraction. The law states that when an x-ray is an incident onto a crystal surface, with an angle of incidence θ , it will reflect with the same angle of scattering θ when the path difference (d) is a whole number (n), of wavelength (λ), constructive interference will occur.

The intensity of the diffracted X-rays is measured as a function of the diffraction angle 2θ and the specimen's orientation. This diffraction pattern is used to identify the specimen's crystalline phases and to measure its structural, properties. XRD is non-destructive and does not require elaborate sample preparation, which partly explains the wide usage of XRD method in materials characterization diffraction peak positions are accurately measured with XRD, which makes it the best method for characterizing homogeneous and inhomogeneous strains.

Homogeneous or uniform elastic strain shifts the diffraction peak positions. From the shift in peak positions, one can calculate the shift in d -spacing, which is the result of the change of lattice constants under a strain. Inhomogeneous strains vary from crystallite to crystallite or within a single crystallite and this causes a broadening of the diffraction peaks that increase with $\sin\theta$. Peak broadening is also caused by the finite size of crystallites, but here the broadening is independent of $\sin\theta$

. When both crystallite size and inhomogeneous strain contribute to the peak width, these can be separately determined by careful analysis of peak shapes.

2.3.1.2 POWDER X RAY DIFFRACTION

X-ray powder diffraction (XRD) is a rapid analytical technique primarily used for phase identification of a crystalline material and can provide information on unit cell dimensions. The analysed material is finely ground, homogenized, and average bulk composition is determined.

In powder X-ray diffraction, the diffraction pattern is obtained from a powder of the material, rather than an individual crystal. Powder diffraction is often easier and more convenient than single crystal diffraction since it does not require individual crystals be made. Powder X-ray diffraction (XRD) also obtains a diffraction pattern for the bulk material of a crystalline solid, rather than of a single crystal, which doesn't necessarily represent the overall material.[18]

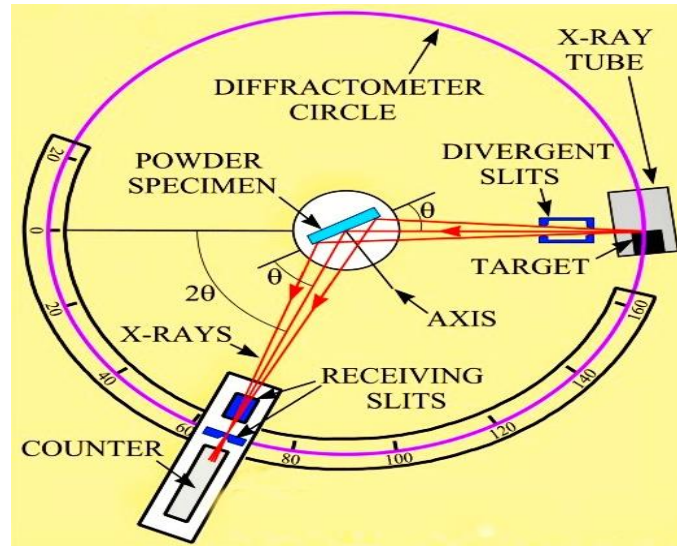


Figure 2.8 Powder XRD

A diffraction pattern can also be used to determine and refine the lattice parameters of a crystal structure. A theoretical structure can also be refined using a method known as Rietveld refinement. The particle size of the powder can also be determined by using the Scherrer formula, which relates the particle size to the peak width. The Scherrer formula is

$$t = \frac{0.9\lambda}{(\sqrt{(BM^2) - BS^2} \cos\theta)} \quad (4)$$

where

λ is the x-ray wavelength, BM is the observed peak width, BS is the peak width of a crystalline standard, and θ is the angle

of diffraction.

2.3.1.3 INSTRUMENTATION

X-ray diffractometers consist of three basic elements: an X-ray tube, a sample holder, and an X-ray detector. When an X-ray is shined on a crystal, it diffracts in a pattern characteristic of the structure. X-rays are generated in a cathode ray tube by heating a filament to produce electrons, accelerating the electrons toward a target by applying a voltage, and bombarding the target material with electrons. When electrons have sufficient energy to dislodge inner shell electrons of the target material, characteristic X-ray spectra are produced.

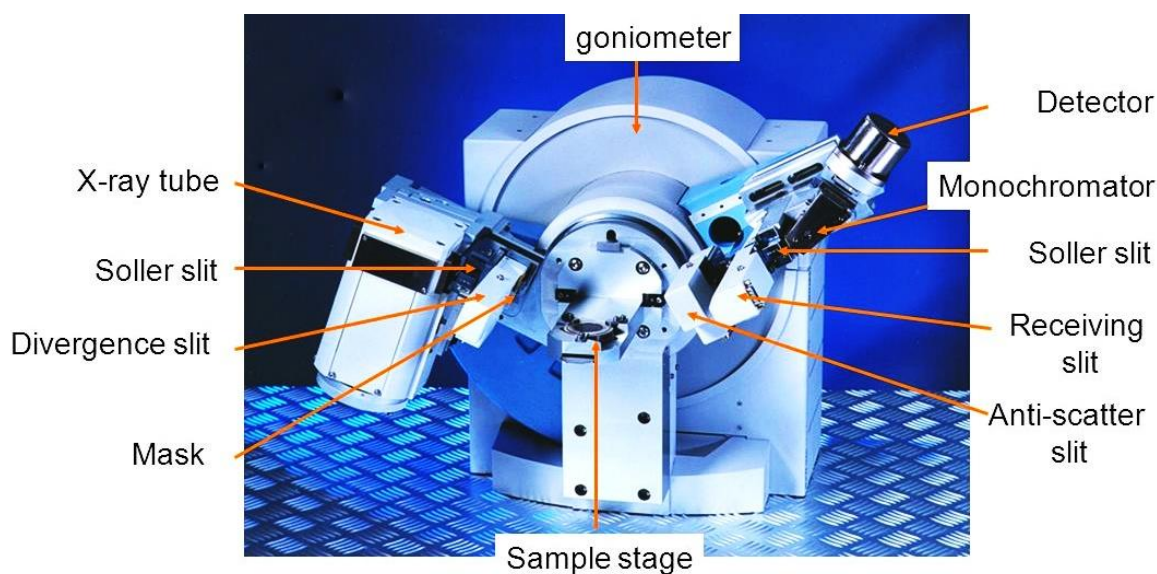


Figure 2.9 – Powder XRD Instrumentation set up[19]

As the sample and detector are rotated, the intensity of the reflected X-rays is recorded. The geometry of an X-ray diffractometer is such that the sample rotates in the path of the collimated X-ray beam at an angle θ while the X-ray detector is mounted on an arm to collect the diffracted X-rays and rotates at an angle of 2θ . The instrument used to maintain the angle and rotate the sample is termed a goniometer. For typical powder patterns, data is collected at 2θ from $\sim 5^\circ$ to 70° , angles that are present in the X-ray scan. When the geometry of the incident X-rays impinging the sample satisfies the Bragg Equation, constructive interference occurs and a peak in intensity occurs. A detector records and processes this X-ray signal and converts the signal to a count rate which is then output to a device such as a printer or computer monitor.

2.3.1.4 APPLICATIONS OF POWDER XRD

X-ray powder diffraction is most widely used for the identification of unknown crystalline materials (e.g., minerals, inorganic compounds). Some of them are

- Determination of unknown solids is critical to studies in geology, environmental science, material science, engineering and biology.
- Identification of fine-grained minerals such as clays and mixed layer clays that are difficult to determine optically
- Determination of unit cell dimensions
- Measurement of sample purity
- Determine of modal amounts of minerals (quantitative analysis).

2.3.2 UV VISIBLE SPECTROSCOPY

Spectroscopy is the branch of science dealing the study of interaction of electromagnetic radiation with matter. Spectroscopy is the most powerful tool available for the study of atomic & molecular structure and is used in the analysis of a wide range of samples. Science Academies This technique begins from Issac Newton's experiment (1666-1672), which he defined the term 'spectrum' to describe the consecutive colours derived from the dispersion of white light through a prism. Later it was explained as any interaction of electromagnetic waves with matter. In early 19thcentury, Joseph von Fraunhofer made experimental advances with dispersive spectrometers that enabled spectroscopy to become a more precise, quantitative and scientific technique. [20]

- Atomic Spectroscopy: This Spectroscopy is concerned with the interaction of electromagnetic radiation with atoms are commonly in the lowest energy state called as grown state.
- Molecular Spectroscopy; This Spectroscopy deals with the interaction of electromagnetic radiation with molecule.

2.3.2.1 BASIC IDEAS OF UV VISIBLE SPECTROSCOPY

UV-VIS spectroscopy is considered as the most important spectrometric technique that is most widely used for the analysis of variety of compounds. This technique works on the basis of the measurement of interaction of electromagnetic radiations (EMR) with matter at particular wavelength that measures the number of discrete wavelengths of UV or visible light that are absorbed by or transmitted through a sample in comparison to a reference or blank sample.

This property is influenced by the sample composition, potentially providing information on what is in the sample and at what concentration. Light has a certain amount of energy which is inversely proportional to its wavelength. A specific amount of energy is needed to promote electrons in a substance to a higher energy state which we can detect as absorption. Electrons in different bonding environments in a substance require a different specific amount of energy to promote the electrons to a higher energy state. This is why the absorption of light occurs for different wavelengths in different substances. Humans are able to see a spectrum of visible light, from approximately 380 nm, which we see as violet, to 780 nm, which we see as red. UV light has wavelengths shorter than that of visible light to approximately 100 nm. Therefore, light can be described by its wavelength, which can be useful in UV-Vis spectroscopy to analyse or identify different substances by locating the specific wavelengths corresponding to maximum absorbance.

When a photon having sufficient energy reaches an object, the object receives and absorbs the energy, which allows the electron to attain a higher energy state. The amount of radiation or photons absorbed results in the formation of the absorption spectrum, which will be measured in terms of absorbance.

The absorbance of a compound depends on the number of excited electrons from the ground state, which is dependent on the concentration or number of molecules in the sample. The absorbance of radiation by a compound produces a distinct spectrum, which is helpful in serving as a marker or identifier of the compound. The easier the electrons get excited, the longer the wavelength of the light, the compound can absorb.

Four possible types of interactions or transitions can be observed. They are ($\pi-\pi^*$, $n-\pi^*$, $\sigma-\sigma^*$, and $n-\sigma^*$). The order of the interaction according to the energy is as follows: $\sigma-\sigma^* > n-\sigma^* > \pi-\pi^* > n-\pi^*$. The spectrum arises from electron transition in a molecule from a lower level to a higher level.

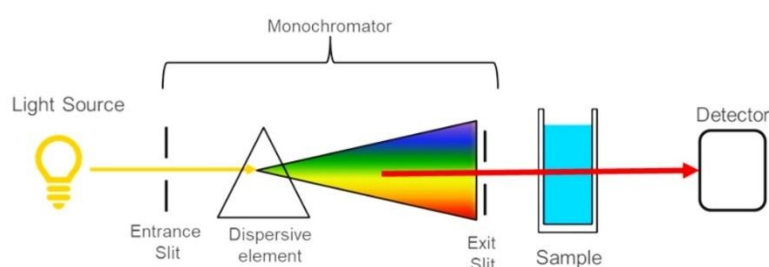


Figure 2.10 - UV visible Spectroscopy Principle

A spectrophotometer is able to record the amount of absorption by a sample at different wavelengths in the UV and visible wavelength range. The plot of absorbance (A) versus wavelength (λ) is called a spectrum. During excitation, the atoms in the bond of molecules merge to form molecular orbitals, which are occupied by electrons of different energy levels. The electrons get excited from the highest occupied molecular orbital (HOMO) to the lowest occupied molecular orbital (LOMO). The resulting spot is called the excited state or antibonding state.

2.3.2.2 INSTRUMENTATION

Ultraviolet-visible (UV-Vis) spectrophotometer is used to quantify and qualify samples by the means of UV and visible light (mainly 200 to 900 nm)

There are a variety of variations to the UV-Vis spectrophotometer. The basic components of UV visible spectrometer include a light source, monochromator or filters, sample holder, Amplifier, detector and recording devices. xenon light source can be employed as a high-intensity light source that can be used in both visible and ultraviolet ranges. A deuterium lamp can be the standard lamp that emits UV light. Because two sources of light are required to cover both UV light wavelength and the visible, the source of light inside the instrument needs to change when measuring.

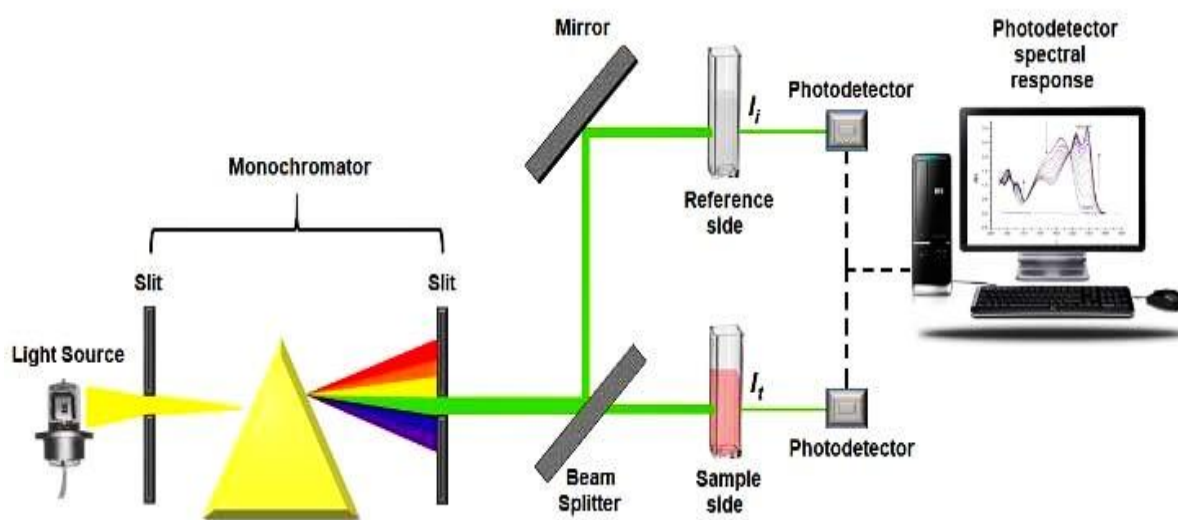


Figure 2.11 - Schematic representation of the dual-beam UV-VIS spectrometer.

Monochromators separate light into a small band of wavelengths. It's typically constructed using diffraction gratings, which can be rotated to select angles for reflection and incoming to choose the length of the light. The wavelength selector that is utilized for the spectrometer light will then pass through the sample. In all analyses the measurement of a reference sample which

is often called “the “blank sample”, such as a cuvette containing similar solvents that was used for the preparation of the specimen is vital. The signal from the reference sample can then be used by the instrument in order to determine the actual absorbance that the analyses absorb.

After the light has passed through the sample, a detector is used to convert the light into a readable electronic signal. Generally, detectors are based on photoelectric coatings or semiconductors. A photoelectric coating ejects negatively charged electrons when exposed to light. When electrons are ejected, an electric current proportional to the light intensity is generated. A photomultiplier tube (PMT) is one of the more common detectors used in UV-Vis spectroscopy. After the electric current is generated from whichever detector was used, the signal is then recognized and output to a computer or screen.



Figure 2.12 - UV Visible Spectrometer[21]

UV-Vis spectroscopy information is usually presented as a graph of absorbance, optical density or transmittance as a function of wavelength. The intensity of light can be reasonably expected to be quantitatively related to the amount of light absorbed by the sample. In UV-Vis spectroscopy, the wavelength corresponding to the maximum absorbance of the target substance is chosen for analysis. This choice ensures maximum sensitivity because the largest response is obtained for a certain a
alite concentration.

2.3.2.3 APPLICATIONS OF UV VISIBLE SPECTROSCOPY

- **Detection of impurities** - UV visible spectroscopy can be used for the detection of impurities present in organic molecules. Additional peaks can be observed due to impurities in the sample, and it can be compared with that of standard raw material.
- **Qualitative & Quantitative Analysis:** It is used for characterizing aromatic compounds and conjugated olefins. It can be used to find out molar concentration of the solute under study.
- **DNA and RNA analysis in microbiology** - Quickly verifying the purity and concentration of RNA and DNA is one particularly widespread application of UV Visible Spectroscopy.
- **Pharmaceutical Research** - Processing UV-Vis spectra using mathematical derivatives allows overlapping absorbance peaks in the original spectra to be resolved to identify individual pharmaceutical compounds.

2.3.3 RAMAN SPECTROSCOPY

Raman spectroscopy is a spectroscopic technique used to detect vibrational, rotational, and other states in a molecular system, capable of probing the chemical composition of materials. It is based on the Raman effect, which was first identified by the Indian physicist Chandrasekhara Venkata Raman in 1928. The Raman effect is based on scattering of light, which includes both

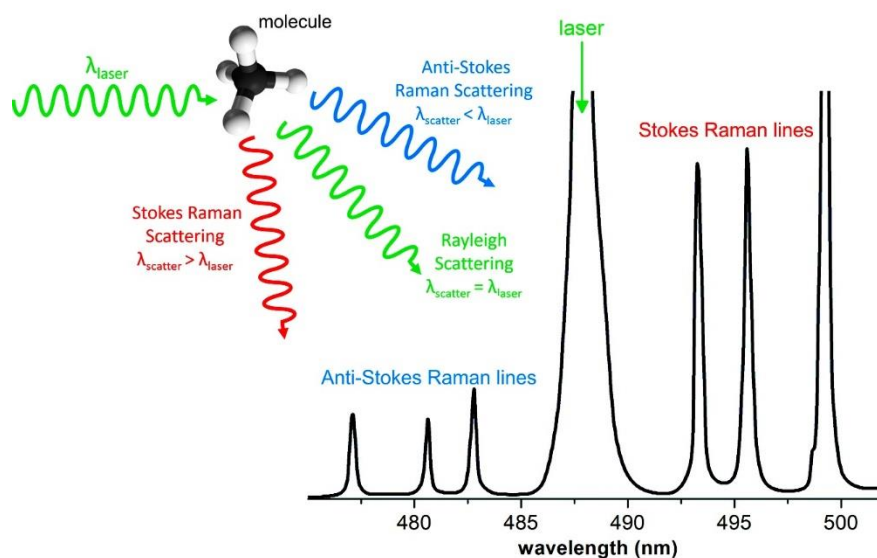


Figure 2.13 – Rayleigh and Raman Scattering in molecules

elastic (Rayleigh) scattering at the same wavelength as the incident light, and inelastic (Raman) scattering at different wavelengths, due to molecular vibrations. When light interacts with molecules in a gas, liquid, or solid, the vast majority of the photons are dispersed or scattered at the same energy as the incident photons. This is described as elastic scattering, or Rayleigh scattering. A small number of these photons, approximately 1 photon in 10 million will scatter at a different frequency than the incident photon. This process is called inelastic scattering.

2.3.3.1 PRINCIPLES OF RAMAN SPECTROSCOPY

Raman spectroscopy is widely used in the investigation of cultural heritage materials due to its high spatial resolution (typically in the range of 1 to 10 μm), large amount of obtainable information, non-destructivity and ability to perform in-situ analysis. With Raman spectroscopy it's possible to analyse various materials: minerals, inorganic and organic pigments, binding media, varnishes, ceramics, plastics, textile fibres etc.

Raman spectroscopy is classified as vibrational spectroscopy. In this technique, the sample is exposed to an intense beam of monochromatic light in the frequency range of visible, near-infrared or near-ultraviolet region. The electromagnetic radiation, interacting with a substance, can be transmitted, absorbed, or scattered. When the monochromatic radiation is scattered by molecules, the majority of the radiation undergoes the common Rayleigh scattering. However, a small fraction of the scattered radiation is observed to have a slightly different frequency from that of the incident radiation. This is known as the Raman effect. The dominant Stokes lines have a lower frequency (longer wavelength) than the initial radiation, whereas the weaker anti-Stokes lines have a higher frequency (shorter wavelength). The frequency shifts are virtually independent of the excitation wavelength and are characteristic of the particular substance/molecule. The phenomenon of Raman scattering is possible on the basis of classical considerations. When a molecule is placed in an electric field, polarization of the medium takes place as the negatively charged electron cloud is being attracted towards the positive pole and the positively charged nuclei get attracted towards the negative pole. The polarization P so induced is proportional to the applied electric field (E)

$$P = \alpha E \quad (5)$$

The constant of proportionality α is the Polarizability of the molecule. The polarization does induced contain the three distinct frequency components

- $V = V_0$ - Rayleigh Line
- $V = V_0 - V_m$ - Raman Stokes Lines
- $V = V_0 + V_m$ - Raman anti-Stokes Lines

According to quantum theory, radiation has both particle and wave nature. If a radiation of frequency V_0 undergo collision with molecules and the collision is perfectly elastic, there will not be any exchange of energy between the photon and the molecule. However, there will be exchange of energy between the two if the collision is inelastic. The molecule can gain or loose energy equal to the energy difference ΔE between the two allowed states.

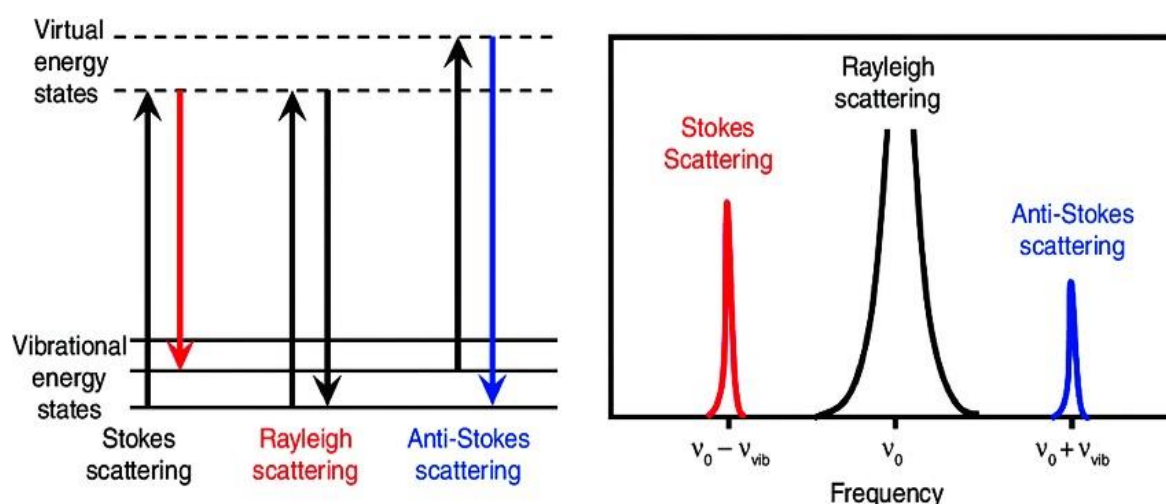


Figure 2.14 - Energy level diagram showing Rayleigh and Raman lines.

The intensity of spectral lines depends on number of factors, the most important factor being the initial population of the state from which transition originate. Based on Boltzmann distribution for the population in states, the intensity ratio of Stokes (I_s) to anti-Stokes (I_{as}) lines is given by

$$\frac{I_s}{I_{as}} = \frac{(V_0 + V_m)^2}{(V_0 - V_m)^2} \exp(hV_m/KT) \quad (6) \text{Where}$$

K is the Boltzmann constant and T is the temperature in Kelvin. Anti-stokes lines have much less intensity than stokes lines.

In Raman spectroscopy, sample is placed in the laser beam and the scattered radiation is collected and analysed. Raman spectrometer measures the wavelength-dependent intensity of the inelastically scattered light. The obtained Raman spectra are essentially vibrational spectra. Raman spectrum arises in a different manner and the rules are different. It turns out that a vibration is Raman-active, if the polarizability of the molecule changes during the vibration and Raman inactive, if Polarizability of the molecule doesn't change. Raman spectra often provide complementary information to IR spectra.[22]

2.3.3.2 INSTRUMENTATION

There are two types of Raman spectrometers: dispersive spectrometers and interferometer containing Fourier-transform Raman spectrometers (FT-Raman). In Raman spectroscopy, the choice of excitation wavelength and intensity is very important. Different wavelengths are suitable for the analysis of different types of material. The wavelength will affect the Raman intensity, spatial resolution, background fluorescence, and potential damage to the sample. Almost exclusively lasers are used as excitation sources, because they are highly monochromatic, give high-intensity radiation and can be efficiently focused due to their high coherence. Only continuous wave (CW) lasers are used, as pulsed lasers easily damage the sample.

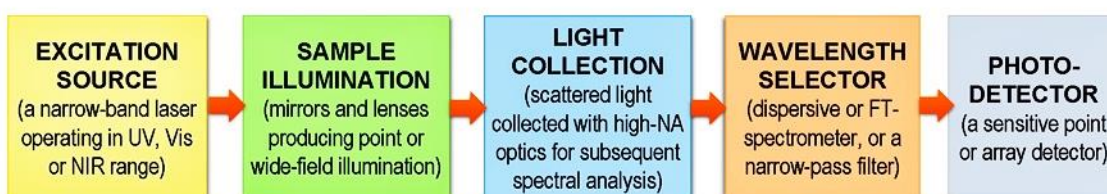


Figure 2.15 – Block diagram of Raman Spectrometer

Raman scattering efficiency decreases with increasing excitation wavelength as λ^{-4} . However, short-wavelength lasers more easily induce fluorescence, absorb in the sample or cause other undesirable effects due to their high photon energy. Hence, most common laser wavelengths in Raman spectroscopy are in the visible and NIR region (such as 633 or 785 nm) which offer low fluorescence whilst retaining relatively high Raman intensity.[22]

2.3.3.2.1 DISPERSIVE RAMAN SPECTROMETER

Dispersive spectrometer utilizes a diffraction grating to angularly disperse the light. As a result, at the detector plane, different wavelengths become spatially separated. Nevertheless, prior to entering the spectrometer, the incoming light should go through a special edge or notch filter to suppress the primary (Raman-scattered) light and thereby reduce the scattering inside the spectrometer. A matrix detector is used to record the dispersed spectrum. Typically, a silicon-based cooled CCD is used, which is very sensitive in the visible and NIR region (up to 1100 nm).

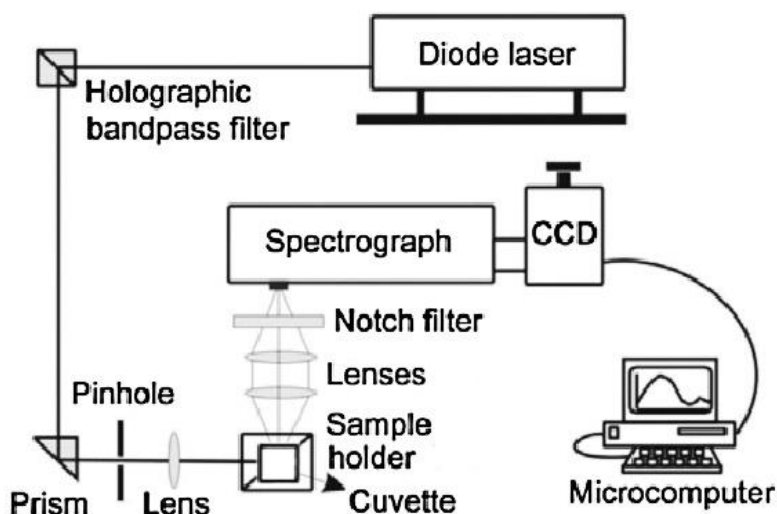


Figure 2.16 - Dispersive Raman Spectrometer

2.3.3.2.2 FT RAMAN SPECTROMETER

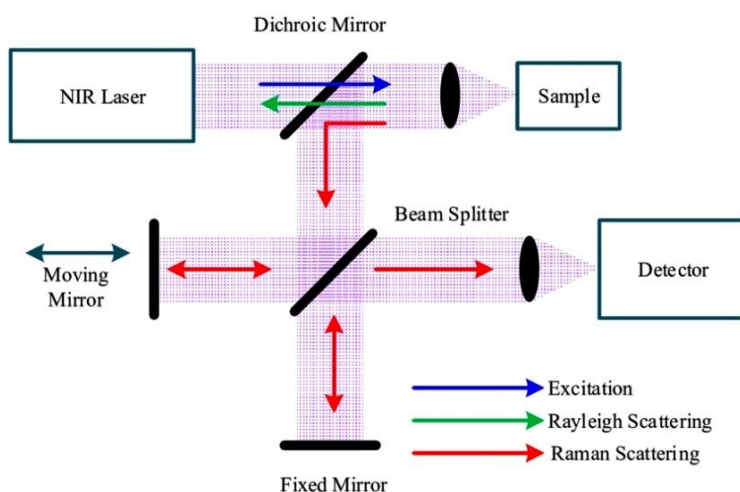


Figure 2.17 - FT Raman Spectrometer

FT-Raman spectrometers were introduced in the late 1980s. Their operating principle is similar to that of FTIR spectrometers and is based on an interferometer. As the Raman-scattered light enters the instrument, the interferometer selectively modulates the individual spectral components by systematically changing an optical path length difference. The resulting beam of light is recorded by a point detector.[23]

FT-Raman is superior to a dispersive instrument in the near-IR region beyond 1000 nm. Commonly, the 1064 nm laser excitation along with germanium or indium gallium arsenide (InGaAs) detector is used. They also offer excellent wavelength accuracy and can potentially combine IR absorption and Raman measurement capacity in single instrument. However, FT-Raman frequently needs to use high laser intensities due to the reduced Raman scattering efficiency at longer wavelengths, which may damage the sample.

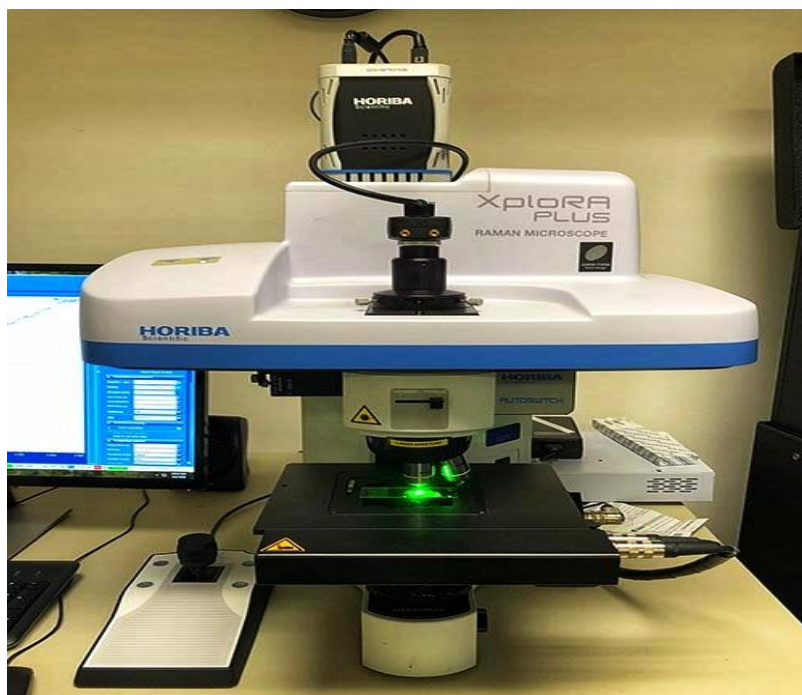


Figure 2.18 – Laboratory Raman Spectrometer

2.3.3.3 APPLICATIONS OF RAMAN SPECTROSCOPY

There are a huge number of applications of Raman spectroscopy.

- **Measuring/mapping stress** – Raman spectroscopy can be used to measure stress and strain in materials. Tensile strain increases the length of the bonds and the tension in them, hence changing the frequency of the phonons. It therefore causes a shift in the observed Raman bands towards lower wavenumbers.
- **Process monitoring** - Raman spectroscopy is a non-destructive process and can be used to monitor industrial processes. The advantage is that the light to be monitored can be sent down fibre-optics, so that the Raman equipment can be located some distance away from the actual processing.
- In solid-state physics, Raman spectroscopy is used to characterize materials, measure temperature, and find the crystallographic orientation of a sample. As with single molecules, a solid material can be identified by characteristic phonon modes. Information on the population of a phonon mode is given by the ratio of the Stokes and anti-Stokes intensity of the spontaneous Raman signal. Raman spectroscopy can also be used to observe other low frequency excitations of a solid.
- In nanotechnology, a Raman microscope can be used to analyse nanowires to better understand their structures, and the radial breathing mode of carbon nanotubes is commonly used to evaluate their diameter.
- Raman spectroscopy has a wide variety of applications in biology and medicine. The technique has confirmed the existence of low-frequency phonons in proteins and DNA, promoting studies of low-frequency collective motion.[22]

REFERENCE

- [1] Eman Assirey Taibah University, “Ideal Cubic Perovskite Structure”.
- [2] E. A. R. Assirey, “Perovskite synthesis, properties and their related biochemical and industrial application,” *Saudi Pharmaceutical Journal*, vol. 27, no. 6. Elsevier B.V., pp. 817–829, Sep. 01, 2019. doi: 10.1016/j.jsps.2019.05.003.
- [3] “Perovskite Crystal.” <https://en.wikipedia.org/>
- [4] “Lev Perovski.” https://www.wikiwand.com/en/Lev_Perovski
- [5] S. C. Watthage, Z. Song, A. B. Phillips, and M. J. Heben, “Evolution of perovskite solar cells,” in *Perovskite Photovoltaics: Basic to Advanced Concepts and Implementation*, Elsevier, 2018, pp. 43–88. doi: 10.1016/B978-0-12-812915-9.00003-4.
- [6] E. A. R. Assirey, “Perovskite synthesis, properties and their related biochemical and industrial application,” *Saudi Pharmaceutical Journal*, vol. 27, no. 6. Elsevier B.V., pp. 817–829, Sep. 01, 2019. doi: 10.1016/j.jsps.2019.05.003.
- [7] “Classification of Perovskites.” doi: [10.1016/j.jsps.2019.05.003](https://doi.org/10.1016/j.jsps.2019.05.003)
- [8] N. F. Atta, A. Galal, and E. H. El-Ads, “Perovskite Nanomaterials – Synthesis, Characterization, and Applications,” in *Perovskite Materials - Synthesis, Characterisation, Properties, and Applications*, InTech, 2016. doi: 10.5772/61280.
- [9] L. Chouhan, S. Ghimire, C. Subrahmanyam, T. Miyasaka, and V. Biju, “Synthesis, optoelectronic properties and applications of halide perovskites,” *Chemical Society Reviews*, vol. 49, no. 10. Royal Society of Chemistry, pp. 2869–2885, May 21, 2020. doi: 10.1039/c9cs00848a.
- [10] S. S. Rong, M. B. Faheem, and Y. B. Li, “Perovskite single crystals: Synthesis, properties, and applications,” *Journal of Electronic Science and Technology*, vol. 19, no. 2, pp. 1–18, 2021, doi: 10.1016/J.JNLEST.2021.100081.
- [11] R. Gupta *et al.*, “Room temperature synthesis of perovskite (MAPbI₃) single crystal by anti-solvent assisted inverse temperature crystallization method,” *J Cryst Growth*, vol. 537, May 2020, doi: 10.1016/j.jcrysgr.2020.125598.
- [12] M. T. Ha, L. van Lich, Y. J. Shin, S. Y. Bae, M. H. Lee, and S. M. Jeong, “Improvement of SiC crystal growth rate and uniformity via top-seeded solution growth under external static magnetic field: A numerical investigation,” *Materials*, vol. 13, no. 3, Feb. 2020, doi: 10.3390/ma13030651.
- [13] H. Shen, R. Nan, Z. Jian, and X. Li, “Defect step-controlled growth of perovskite MAPbBr₃ single crystal,” *J Mater Sci*, vol. 54, no. 17, pp. 11596–11603, Sep. 2019, doi: 10.1007/s10853-019-03710-6.
- [14] “photodetector.” <https://www.sciencedirect.com>
- [15] S. Adjokatse, H. H. Fang, and M. A. Loi, “Broadly tunable metal halide perovskites for solid-state light-emission applications,” *Materials Today*, vol. 20, no. 8. Elsevier B.V., pp. 413–424, Oct. 01, 2017. doi: 10.1016/j.mattod.2017.03.021.

- [16] R. Surabhi, K. Bhat, A. Batra, A. Chilvery, and M. Aggarwal, "Synthesis, Purification, Crystal Growth and Characterization of Lead Iodide (PbI_2) Purified by a Low-Temperature Technique," *Adv Sci Eng Med*, vol. 6, no. 12, pp. 1269–1273, Jan. 2015, doi: 10.1166/ase.2014.1637.
- [17] "X-Ray Diffraction." <https://doi.org/10.1016/j.jnlest.2021.100081>
- [18] "Powder XRD." <https://pubmed.ncbi.nlm.nih.gov/>
- [19] L. S. U. C. M. C. E. M. U. Barbara L Dutrow, "Powder XRD instrumentation."
- [20] P. Justin Tom, "UV Visible spectroscopy."
- [21] "UV-1280 UV-Vis Spectrophotometer from Shimadzu Scientific Instruments."
- [22] S. S. Rong, M. B. Faheem, and Y. B. Li, "Perovskite single crystals: Synthesis, properties, and applications," *Journal of Electronic Science and Technology*, vol. 19, no. 2, pp. 1–18, 2021, doi: 10.1016/J.JNLEST.2021.100081.
- [23] "Energy-level diagram showing the states involved in Raman spectra."
- [24] Y. Yamada *et al.*, "Dynamic Optical Properties of $\text{CH}_3\text{NH}_3\text{PbI}_3$ Single Crystals As Revealed by One- and Two-Photon Excited Photoluminescence Measurements," *J Am Chem Soc*, vol. 137, no. 33, pp. 10456–10459, 2015, doi: 10.1021/jacs.5b04503.
- [25] P. Fan *et al.*, "High-performance perovskite $\text{CH}_3\text{NH}_3\text{PbI}_3$ thin films for solar cells prepared by single-source physical vapour deposition," *Sci Rep*, vol. 6, no. 1, p. 29910, 2016, doi: 10.1038/srep29910.
- [26] P. M and P. Predeep, "Hybrid perovskite single crystal with extended absorption edge and environmental stability: Towards a simple and easy synthesis procedure," *Mater Chem Phys*, vol. 239, no. April 2019, p. 122084, 2020, doi: 10.1016/j.matchemphys.2019.122084.
- [27] R. E. Aderne *et al.*, "On the energy gap determination of organic optoelectronic materials: The case of porphyrin derivatives," *Mater Adv*, vol. 3, no. 3, pp. 1791–1803, 2022, doi: 10.1039/d1ma00652e.
- [28] S. Kim *et al.*, "A band-gap database for semiconducting inorganic materials calculated with hybrid functional," *Sci Data*, vol. 7, no. 1, pp. 1–6, 2020, doi: 10.1038/s41597-020-00723-8.
- [29] D. Donnelly and J. Sadler, "Optical Mapping of Organohalide Lead Perovskite Films By by," no. May, 2018.
- [30] T. Ben-uliel *et al.*, "Raman scattering obtained from laser excitation of MAPbI_3 single crystal," *Appl Mater Today*, vol. 19, p. 100571, 2020, doi: 10.1016/j.apmt.2020.100571.
- [31] R. G. Niemann *et al.*, "Halogen Effects on Ordering and Bonding of $\text{CH}_3\text{NH}_3 + \text{in } \text{CH}_3\text{NH}_3\text{PbX}_3$ ($\text{X} = \text{Cl}, \text{Br}, \text{I}$) Hybrid Perovskites: A Vibrational Spectroscopic Study," vol. 3, 2016, doi: 10.1021/acs.jpcc.5b11256.

- [32] J. Downloaded *et al.*, “Organic – inorganic interactions of single crystalline organolead halide perovskites studied by Raman spectroscopy †,” pp. 14–16, 2016, doi: 10.1039/c6cp01723a.
- [33] Y. Liu *et al.*, “20-mm-Large Single-Crystalline Formamidinium-Perovskite Wafer for Mass Production of Integrated Photodetectors,” *Adv Opt Mater*, vol. 4, no. 11, pp. 1829–1837, 2016, doi: 10.1002/adom.201600327.
- [34] Z. Yang *et al.*, “Unraveling the Exciton Binding Energy and the Dielectric Constant in Single-Crystal Methylammonium Lead Triiodide Perovskite,” *Journal of Physical Chemistry Letters*, vol. 8, no. 8, pp. 1851–1855, 2017, doi: 10.1021/acs.jpclett.7b00524.

CHAPTER – 3

RESULTS AND DISCUSSION

Methylammonium lead iodide (MAPbI_3) single crystal have been prepared by inverse temperature crystallisation method as mentioned in the previous chapter. A 12 mm length crystal was obtained and the crystal is subjected to various characterisation methods such as x – ray diffraction, UV- visible spectroscopy and Raman spectroscopy. The charge transport properties of the single crystal was analysed from IV measurements taken using Keithley 2400 source meter by Space Charge Limited (SCLC) method. Methyl ammonium lead halide material is one of the promising candidates for future solar cell technology. The power conversion efficiency (PCE) of perovskites increased from 3.8 % to 22 % in a span of less than a decade. Single crystalline organo-lead halide perovskite has better diffusion length and mobility compared to solution processed perovskite films. So they have high phase and material purity and lesser number of defects.

Inverse Temperature Crystallization (ITC) method is one of the faster methods to grow single crystals of perovskites like MAPbI_3 , comparing with other methods. The method utilises the retrograde solubility of perovskite in specific solvents. Normally the solubility of a given solute in a given solvent increases with temperature but some solutes become less soluble as temperature increases this inverse temperature dependence referred to as retrograde or inverse solubility.

The precursor salts are taken in specific amounts and the sample is prepared using the above prescribed method.

- Molecular weight of MAI = 158.9695 g/mol
Desired final volume of MAI solution = 5 ml
Molarity = 1.23 M
Mass of Methylamine iodide = 2.8352 g
- Molecular weight of PbI_2 = 461.01 g/mol
Desired final volume of PbI_2 = 5 ml
Molarity = 1.23 M
Mass of Lead iodide = 0.9776 g

The results and discussion of various characterisation technique used for the analyses of the sample are given below –

3.1 X- RAY DIFFRACTION STUDIES

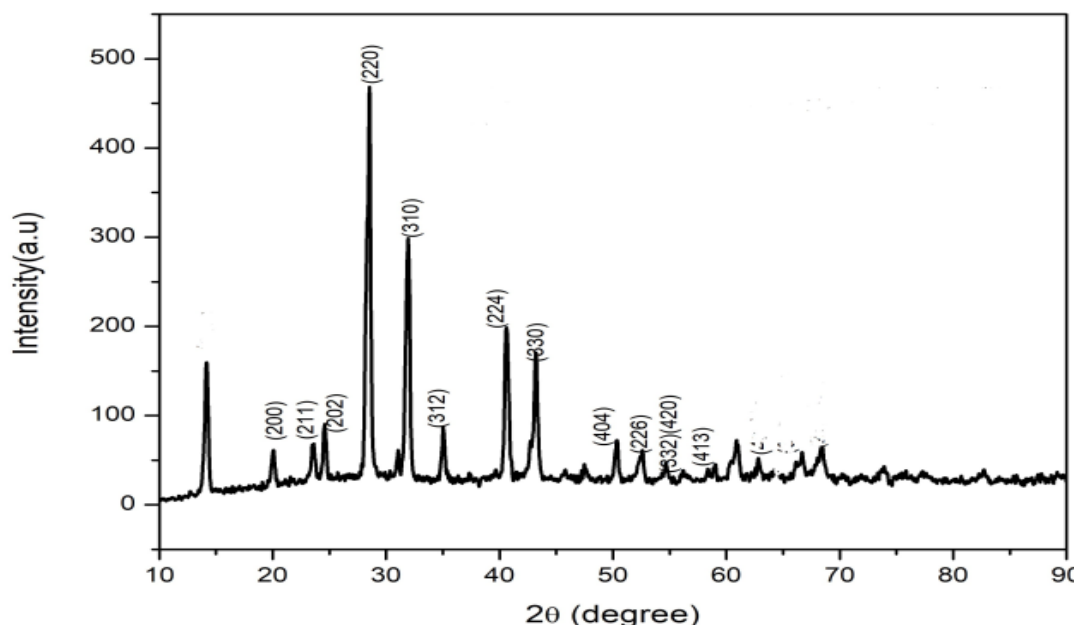


Figure 3.1: Powder XRD of MAPbI₃

Powder X-ray diffraction measurements were performed on the ground MAPbI₃ single crystal, to further assert the single crystalline nature and structure of the synthesized single crystal of MAPbI₃. XRD data so collected are compared with ICSD data (ICSD collection code: 238610) [24] (Figure 1). A set of preferred orientations[25] corresponding to the planes (110), (220), (310), (224), and (330) were observed at 2Θ values, 14.080, 28.440, 31.850, 40.580 and 43.190 of the MAPbI₃ tetragonal structure, respectively. Minor peaks are also present at 2Θ values of 19.920, 23.540, 24.52, 340.940, 50.220 and 52.540 and are assigned to the planes (112), (211), (202), (204), (404), and (336) respectively. This had confirmed that the grown product is MAPbI₃ single crystal having high material and phase purity. Further, no MAI and PbI₂ characteristic peaks are found to be present in the XRD data, indicating the effectiveness of the washing of the grown crystal with isopropanol and diethyl ether to remove the lead iodide impurity.

3.2 UV VISIBLE ABSORPTION SPECTRUM

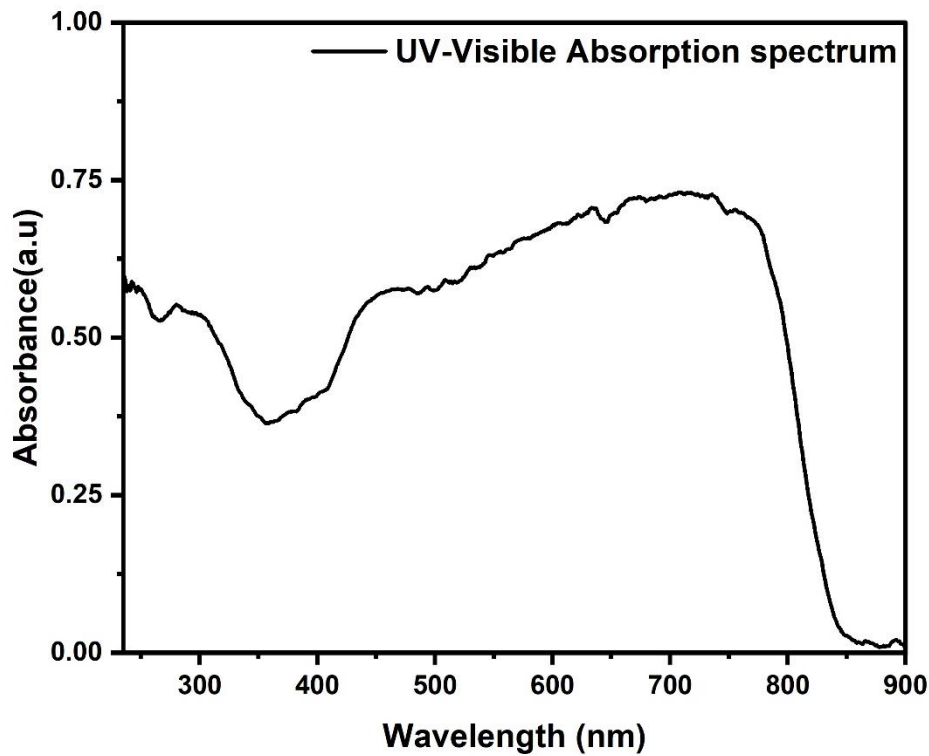


Figure 3.2 : UV-Visible Absorption Spectrum of MAPbI₃

The UV-Visible absorption spectra of single crystal powder were taken in 200-900 nm range using Avaspec 2048 spectrophotometer equipped with halogen and deuterium lamps. Measurements were carried out at room temperature. Figure 1 shows the absorption spectrum of MAPbI₃ single crystals taken in reflection mode. Single crystal possess excellent light harvesting ability in the visible range till 800 nm. So, they can be used as light harvesting material in solar cells. There is a sudden drop in the absorption after 800nm indicating that the material possesses sharp absorption edge. Absorption edge of polycrystalline counterpart is around 790 nm, the red shift [26] in the upper limit of absorption point towards the effectiveness of using single crystals as light harvesting materials in solar cells. Figure 2 shows the Tauc plot for obtaining the bandgap of the material. By using the Tauc plot method, the E_g is determined through a linear extrapolation of the observed trend in the spectral dependence of $(\alpha h\nu)^2$ which intercepts the abscissa axis giving by the photon energies $h\nu$ [27]. By extrapolating the straight-line portion of the curve to the energy axis direct band gap(E_g) is obtained as 1.51 eV. The mathematical expression governing bandgap calculation is given by

$$(\alpha h\nu)^{(1/\gamma)} = B(h\nu - E_g) \quad (1)$$

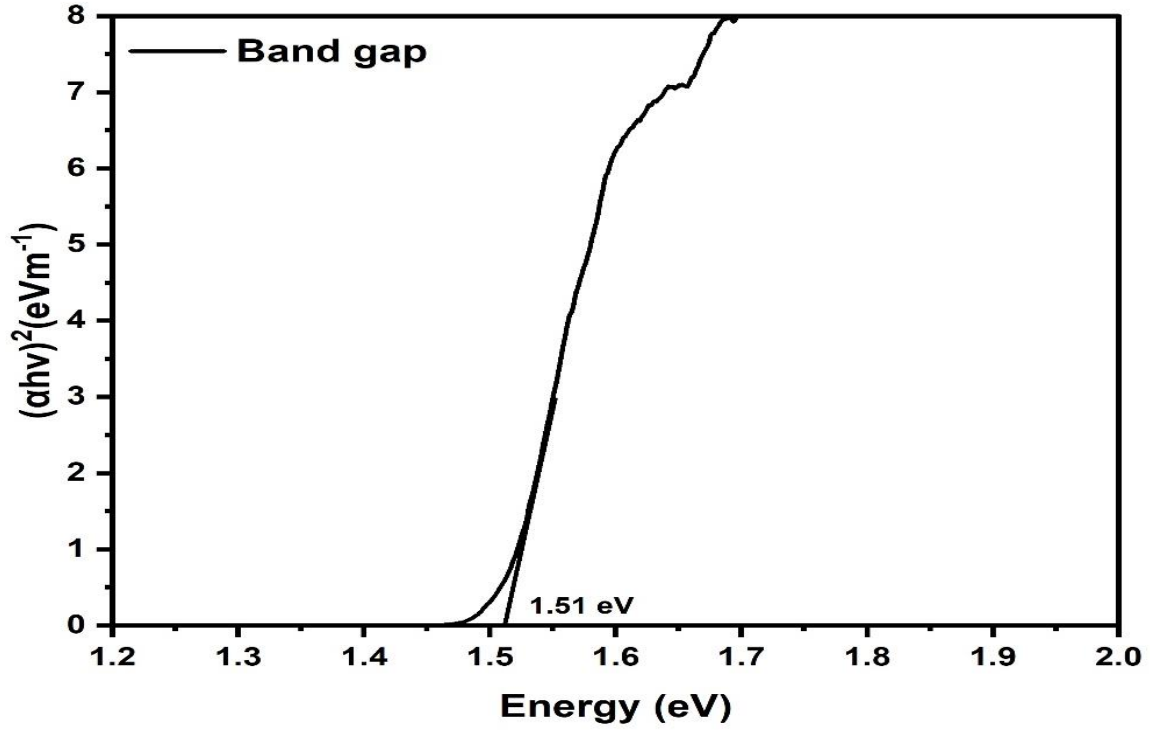


Figure 3.3 : Band gap of MAPbI₃

where h is the Planck constant, ν is the photon's frequency, E_g is the band gap energy, and B is a constant. Also, the energy dependent absorption coefficient,

$$\alpha = 2.303 * \left(\frac{A}{d} \right) \quad (2)$$

where A is the absorbance and d are the internal width of the cuvette for liquid or thickness in case of film. For direct band gap, the value of γ is $\frac{1}{2}$ and for indirect, the value is 2.

Band gap is a fundamental quantity that predicts the usefulness of the material in photovoltaic and energy applications. Usually devices with $E_g \sim 1.3$ eV[28] are used as acceptor material in solar cells according to Schottky Queisser limit. Bandgap of this material comes the category of semiconducting materials.

3.3 RAMAN SPECTRUM ANALYSIS

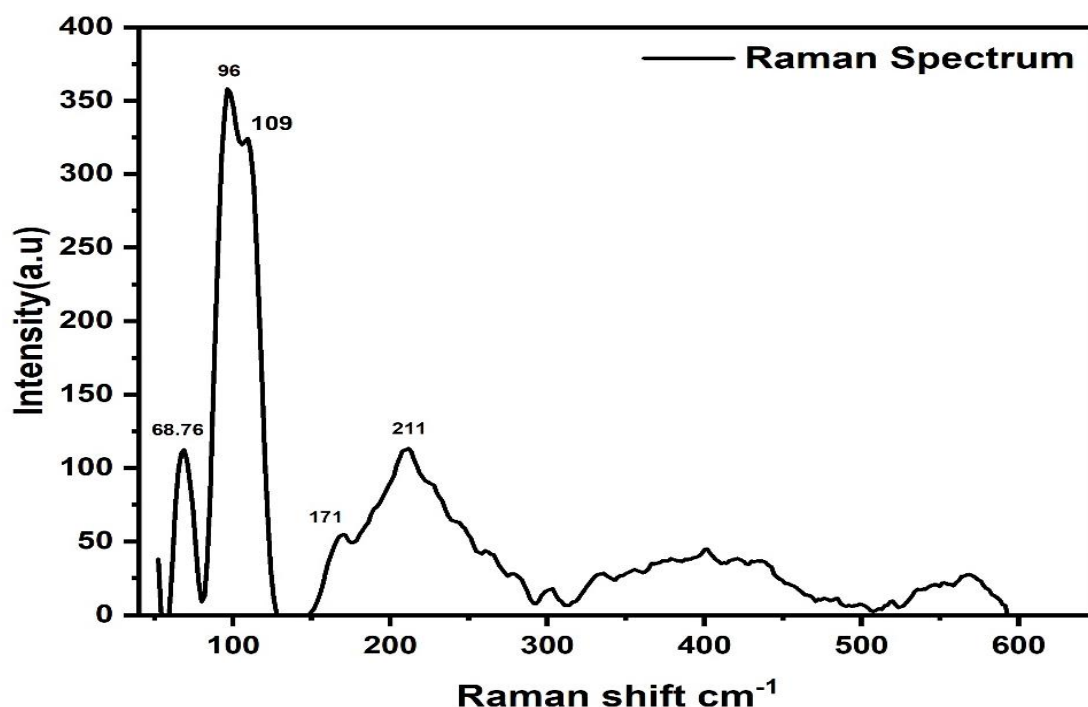


Figure 3.4: Raman Spectrum of MAPbI₃

Raman spectrum is a powerful tool for analysing the structural properties of materials from fingerprint vibrations. Peak position indicates molecular structure, peak height depends on the concentration of the material, peak width is related to crystallinity of the material and peak shifts is a measure of stress[29]. This is the reason why Raman vibrations are usually known as molecular fingerprints. Mainly the peak position indicates functional groups. In the Raman spectrum all samples show a prominent peak around 99 cm⁻¹. The vibrations around 100 cm⁻¹ are due to the Pb-I cage of MAPbI₃[30]. MAPbI₃ single has a vibration around 138 cm⁻¹ due to librational modes of MA cations[30]. Methyl Ammonium Iodide (MAI) have peaks around 1400-1500cm⁻¹ due to asymmetric bending and twisting of NH⁺[31]. The vibrational modes of MA⁺ are highly sensitive to microenvironment[32].

3.4 CHARGE TRANSPORT STUDIES

Charge transport properties of the as grown MAPbI₃ single crystals were analysed by Space Charge Limited Current (SCLC) method. The device structure is shown in figure 3.5 and the log-log plot of the IV characteristics is shown in figure 3.6. A 100 nm thickness copper electrode was thermally deposited on both sides of the MAPbI₃ single crystal, and connections were made by spring-loaded contacts. The ohmic (slope = 1), trap -filled (slope = 3), Child or SCLC region s (slope = 2) are identified from the graph as shown in Figure 8. Three regions firstly a linear ohmic region that can be used for measuring electrical conductivity (σ) at low bias, secondly a trap-filled region for calculating trap state density (n_{trap}) at the middle bias, and finally SCLC trap-free region for estimating charge carrier mobility (μ) at high bias are clearly visible in the I-V curve.

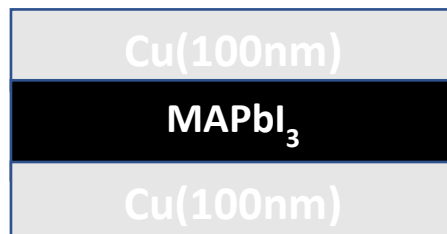


Figure 3.5 : Device structure for IV measurement

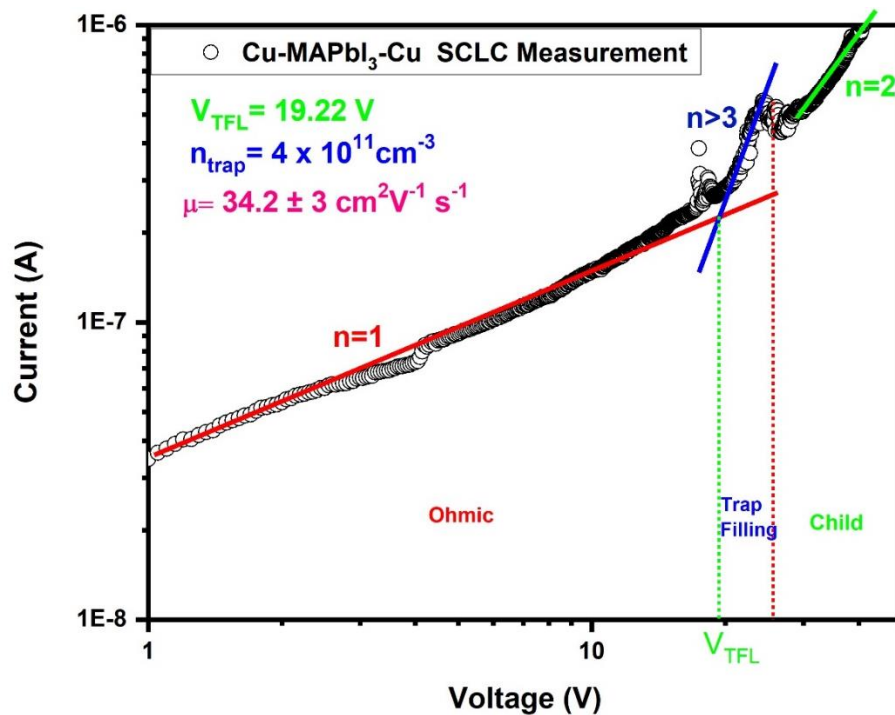


Figure 3.6 : SCLC measurement

The current density J increases linearly with applied voltage V when the voltage is lower than the kink point voltage, revealing an ohmic response. J exhibits a quick nonlinear increase (slope > 3) as the applied voltage reaches the first kink point voltage, indicating that the injected carriers have filled all the trap states. The trap-filled limit voltage V_{TFL} , which is governed by the trap state density n_{trap} , is the applied voltage at the kink point, given by the relation[33] .

$$V_{\text{TFL}} = \frac{e n_{\text{trap}}}{2\epsilon\epsilon_0} d^2 \quad (3)$$

where e is the elementary charge ($1.6 \cdot 10^{-19}$ C), d is the thickness of the single crystal ($d = 2.2$ mm), ϵ_0 is the permittivity of free space ($\epsilon_0 = 8.85 \cdot 10^{12}$ F/m), and ϵ is the relative dielectric constant of MAPbI₃ ($\epsilon = 9.33$ [34]). The calculated trap-state density n_{trap} is $4 \times 10^{11} \text{ cm}^{-3}$ by taking VTFL as 19.22 V.

At higher bias, the current density J shows a quadratic dependence on the voltage V that can be fitted well by the Mott–Gurney law [33].

$$J = \frac{9}{8} \mu \epsilon_0 \epsilon_r \frac{V^2}{d^3} \quad (4)$$

other symbols have the same definition as in previous equation. It was found that the calculated hole transport mobility $\mu = 34.2 \text{ cm}^2/\text{vs}$.

3.5 CONCLUSION

Methyl ammonium lead halide perovskite single crystals were synthesized by Inverse Temperature Crystallization (ITC). Material characterization reports corroborates with previous reported results in the literature. Single crystal possesses' mobility of the order of $34 \text{ cm}^2/\text{Vs}$. These perovskites have excellent optoelectronic properties and light harvesting properties. Charge carrier mobility is an important parameter for enhancing the efficiency of solar cell. Mobility ranges of synthesized single crystals make them excellent candidates for solar cells.

Methylammonium lead iodide perovskite crystal of 12mm in length was synthesised using inverse crystallisation method. The method provides the faster results for the synthesis of perovskite crystal. Various characterisation techniques were used for the proper identification of methylammonium lead iodide perovskite. XRD analysis was carried out for the determination of the structure of the crystal. It was found that MAPbI_3 crystal is tetragonal in shape. In $\text{CH}_3\text{NH}_3\text{PbI}_3$ cubic crystal structure the methylammonium cation (CH_3NH_3^+) is surrounded by PbI_6 octahedra. The Pb ion can migrate through the crystal with an activation energy of 0.6 eV.

The methylammonium cations can rotate within their cages. At room temperature the ions have the CN axis aligned towards the face directions of the unit cells and the molecules randomly change to another of the six face directions on a 3 ps time scale. Growth of a $\text{CH}_3\text{NH}_3\text{PbI}_3$ single crystal in gamma-butyrolactone at 110°C . The yellow colour originates from the lead (II) iodide precursor. The growth rates are $3\text{--}20 \text{ mm}^3/\text{hour}$ for $\text{CH}_3\text{NH}_3\text{PbI}_3$. The resulting crystals are metastable and dissolve in the growth solution when cooled to room temperature. The bandgaps of 1.51 eV for $\text{CH}_3\text{NH}_3\text{PbI}_3$ and carrier mobilities $67 \text{ cm}^2/(\text{V}\cdot\text{s})$. Their thermal conductivity is exceptionally low, $\sim 0.5 \text{ W}/(\text{K}\cdot\text{m})$ at room temperature for $\text{CH}_3\text{NH}_3\text{PbI}_3$.

REFERENCES

- [1] Y. Yamada *et al.*, “Dynamic Optical Properties of $\text{CH}_3\text{NH}_3\text{PbI}_3$ Single Crystals As Revealed by One- and Two-Photon Excited Photoluminescence Measurements,” *J. Am. Chem. Soc.*, vol. 137, no. 33, pp. 10456–10459, 2015, doi: 10.1021/jacs.5b04503.
- [2] P. Fan *et al.*, “High-performance perovskite $\text{CH}_3\text{NH}_3\text{PbI}_3$ thin films for solar cells prepared by single-source physical vapour deposition,” *Sci. Rep.*, vol. 6, no. 1, p. 29910, 2016, doi: 10.1038/srep29910.
- [3] P. M and P. Predeep, “Hybrid perovskite single crystal with extended absorption edge and environmental stability: Towards a simple and easy synthesis procedure,” *Mater. Chem. Phys.*, vol. 239, no. April 2019, p. 122084, 2020, doi: 10.1016/j.matchemphys.2019.122084.
- [4] R. E. Aderne *et al.*, “On the energy gap determination of organic optoelectronic materials: The case of porphyrin derivatives,” *Mater. Adv.*, vol. 3, no. 3, pp. 1791–1803, 2022, doi: 10.1039/d1ma00652e.
- [5] S. Kim *et al.*, “A band-gap database for semiconducting inorganic materials calculated with hybrid functional,” *Sci. Data*, vol. 7, no. 1, pp. 1–6, 2020, doi: 10.1038/s41597-020-00723-8.
- [6] D. Donnelly and J. Sadler, “Optical Mapping of Organohalide Lead Perovskite Films By by,” no. May, 2018.
- [7] T. Ben-uliel *et al.*, “Raman scattering obtained from laser excitation of MAPbI_3 single crystal,” *Appl. Mater. Today*, vol. 19, p. 100571, 2020, doi: 10.1016/j.apmt.2020.100571.
- [8] R. G. Niemann *et al.*, “Halogen Effects on Ordering and Bonding of CH_3NH_3 in $\text{CH}_3\text{NH}_3\text{PbX}_3$ ($\text{X} = \text{Cl}, \text{Br}, \text{I}$) Hybrid Perovskites: A Vibrational Spectroscopic Study,” vol. 3, 2016, doi: 10.1021/acs.jpcc.5b11256.
- [9] J. Downloaded *et al.*, “Organic – inorganic interactions of single crystalline organolead halide perovskites studied by Raman spectroscopy †,” pp. 14–16, 2016, doi: 10.1039/c6cp01723a

SUMMARY AND SCOPE FOR FUTURE STUDY

Methylammonium lead iodide perovskite has been of great concern in recent fields of study. The required single perovskite crystal is made using inverse temperature crystallization method. The interdependence of the structure and property in single crystalline perovskite films is yet to be established to enrich the high-speed photon detection applications. The lower bandgap, larger exciton concentration with reduced recombination, and more effective carrier are difficulties in device applications. gadgets used in industrial settings. To advance this technique, it is necessary to have synthesis control over the orientation and thickness of large-area single-crystal films, pertaining to their incorporation into the photovoltaic devices.

To produce lead free environment all-inorganic perovskites that can pave the way for ambiently stable devices, strategies must be established, and difficulties must be overcome to replace the unstable MA cation and hazardous Pb. Due to their structural relaxations and improved PL intensities, thin 2D perovskite single crystals may be optimal. The use of quasi 2D and hybrid 2D/3D perovskites with Lewis's base surface modifications are attractive candidates for device construction and control. The 2D/3D mixed perovskite single crystals can be used to make more stable single-junction and multi-junction devices by applying the potential improvements. MAPbBr_3 and MAPbI_3 are the organic-inorganic hybrid perovskites that are commonly used for single crystals.

Implementation of high-quality perovskite single crystals in applications like LEDs, PDs, and solar cells not only improves the performance of these devices, but also simplifies their structure and facilitates fabrication by several methods. So, in addition to careful optimization of crystal quality improvement, the development of rational surface passivation techniques is needed the most. Organic-inorganic halide perovskites have a significant impact on photovoltaic devices and the solar-to-Power conversion efficiency is considerably high (~20.1%) compared to the existing organic solar cells and dye-sensitized solar cells. For the past three years, there has been tremendous improvement in photovoltaic efficiency of perovskites, i.e. ~9.7% in 2012 to 20.1% in 2015. Meanwhile, several fabrication approaches, inorganic and organic hole transport materials, and device concepts have been developed for high-performing devices. Nevertheless, some issues need to be addressed to commercialize perovskite solar cells. Particularly, the stability of these cells is not well documented in the literature so far.